NASA CR-145066 62

CRACK PROBLEMS IN CYLINDRICAL AND SPHERICAL SHELLS

BY

F. ERDOGAN

FEBRUARY 1976

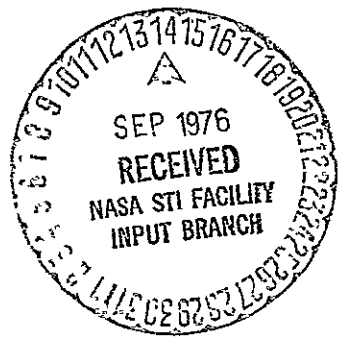

LEHIGH UNIVERSITY
BETHLEHEM, PENNSYLVANIA

THE NATIONAL AERONAUTICS AND SPACE ADMINISTRATION
GRANT NO. NGR 39-007-011

F. Erdogan

5

CRACK PROBLEMS IN CYLINDRICAL AND SPHERICAL SHELLS

5.1 Introduction

Particularly within the past decade the so-called linear fracture mechanics has established itself as a highly satisfactory working tool in studying the phenomena of brittle fracture and fatigue crack propagation in structural solids. The technique appears to be most effective when "plane strain" conditions prevail along the existing crack front. It has also been shown that the stress intensity factor, which is the basic element in the linear fracture mechanics, is the most appropriate correlation parameter in fatigue crack propagation studies of relatively thin-walled plates under membrane loading where the crack is a through crack, and "generalized plane stress" conditions are assumed to exist. The plane assumption here, of course, is an approximation in which the three-dimensional effects resulting from the intersection of the crack plane with the stress-free surfaces of the plate are neglected.* From the view point of practical applications this boundary layer or thickness effect does not appear to be very significant. Therefore, one may be justified in using standard plate or shell theories for studying the fracture problems in thin-walled structures provided the plane of the crack is perpendicular to the surface of the sheet.

With the assumption of linearity, it is known that the relevant information in crack problems may be obtained from a local perturbation problem in which the only external loads are the crack surface tractions. In "thin-walled" structures this would mean that after solving the plate or shell problem under

*See Chapter 2 of this volume for the effect of plate thickness and related approximate techniques.

given external loads by ignoring the crack, the stress intensity factors may be found by using the equal and opposite of the membrane and bending resultants at the location of the crack as the crack surface tractions. Since at the present time linear problems are the only tractable crack problems, the geometry of the particular thin-walled structure must then be such that locally, small deformation plate or linearized shallow shell theories are applicable. At first sight it may appear that in such cases it is sufficient to approximate the structure locally by a flat plate. However, recent studies have shown that local shell curvatures may have a rather considerable effect on the stress intensity factors. Hence, in thin-walled curved structures the crack problem must be considered in conjunction with a shell rather than a plate theory.

Because of the peculiarity of the crack problems in shells, there are analytical limitations regarding the type of problems which can be solved by the existing techniques. Aside from the considerations regarding the linearity of the problem, the two major limitations arise from the geometry and material behavior of the shell. The geometrical factors include the relative size of the crack with respect to the radii of curvature and dimensions of the shell, spatial variation of the curvatures, and the shape and orientation of the crack. The material factors are primarily the anisotropy and nonhomogeneity. In addition to linear elasticity, in the existing solutions [e.g., 1-13] it is assumed that the shell is "infinitely" large, the curvatures are constant (i.e., the shell is a circular cylinder or a sphere), the crack is along a principal plane of curvature, and the material is isotropic and homogeneous. If these assumptions are disregarded, mathematically the problem does not seem to be tractable. Further remarks will be made in this chapter regarding this point. If the material is isotropic and homogeneous, in applications one could obtain

approximate solutions with an acceptable accuracy by approximating local shell-crack geometry with an ideal shell which has a solution, namely a spherical shell with a meridional crack, a cylindrical shell with an axial crack, or a cylindrical shell with a circumferential crack.

From a practical view point the assumption of homogeneity of the material in shells does not seem to be a critical restriction. Even in thin-walled structures made of composites one may easily assume that the gross behavior of the material is homogeneous. However, in practice a mild or strong anisotropy in shells appears to be a rule rather than an exception. Most metallic shells are manufactured through rolling or extrusion process, and hence, are generally mildly anisotropic. Shells which are made of composites such as fiberglass, boron-epoxy, graphite-epoxy, etc., are of course, strongly anisotropic. Since the treatment of anisotropic or, even orthotropic shells is not tractable, it is therefore desirable to have a technique for approximately evaluating the effect of material anisotropy on the critical fracture parameter, namely, the stress intensity factor.

This chapter describes a method of solution for the specially orthotropic shells containing a crack. The method is described by considering symmetric and skew-symmetric problems in cylindrical shells with an axial crack (for details see [14-16]). Its extension to the other two ideal geometries seems to be straightforward. Most of the numerical results given in the chapter, which includes the effect of Poisson's ratio and interaction of two cracks, is, however, on the isotropic shells. The analysis and the results given in this chapter are based on an 8th order linearized shallow shell theory in which Kirchhoff assumption is made with regard to the transverse shear and the

twisting moment on the crack surface. Since there are five traction components on the boundary, to satisfy all the boundary conditions individually a 10th order theory should be used.* Also, since any bending theory is necessarily approximate, one would expect that the shell thickness will have a slight effect on the membrane component and a considerable effect on the bending component of the stress intensity factor.**

5.2 Formulation of the Specially Orthotropic Cylindrical Shell Problem

The linearized bending theory of anisotropic shallow shells dates back to a paper by Ambartsumyan [18] and the detailed treatment of the subject may be found in [19-21]. Referring to Figure 5.1, let an infinitely long orthotropic circular cylindrical shell of elastic constants E_1, ν_1, E_2, ν_2, G_{12}, thickness h, and mean radius R contain an axial through crack of length 2a. Assume that through a proper superposition the problem has been reduced to a local perturbation problem in which the crack surface tractions are the only external loads. Defining the nondimensional orthogonal coordinates in the tangent plane by

$$x_1 = X/a \quad , \quad y_1 = Y/a \tag{5.1}$$

The differential equations for the orthotropic cylindrical shell may be written as

$$D_1\nabla_1^4 w(x_1,x_2) - \frac{a^2}{R}\frac{\partial^2}{\partial x_1^2}F(x_1,x_2) = 0, \tag{5.2a}$$

$$\nabla_2^4 F(x_1,x_2) + \frac{hE_2a^2}{R}\frac{\partial^2}{\partial x_1^2}w(x_1,x_2) = 0, \tag{5.2b}$$

*See Chapter 6 of this volume.

**See Chapter 2 of this volume. See also [17] for cracked plate under bending.

where x_1 and x_2 are the principal directions of orthotropy taken respectively along axial and circumferential directions, F is a stress function, w is the displacement component normal to the shell surface, and the operators ∇_1^4 and ∇_2^4 are defined by

$$\nabla_1^4 = \frac{\partial^4}{\partial x_1^4} + 2\left[\nu_2 + 2(1 - \nu_1\nu_2)\frac{G_{12}}{E_1}\right]\frac{\partial^4}{\partial x_1^2 \partial x_2^2} + \frac{E_2}{E_1}\frac{\partial^4}{\partial x_2^4}, \tag{5.3a}$$

$$\nabla_2^4 = \frac{\partial^4}{\partial x_1^4} + 2\left(\frac{E_2}{2G_{12}} - \nu_2\right)\frac{\partial^4}{\partial x_1^2 \partial x_2^2} + \frac{E_2}{E_1}\frac{\partial^4}{\partial x_2^4}. \tag{5.3b}$$

The notation for the orthotropic elastic constants are defined by the following stress strain relations:

$$\varepsilon_{11} = \frac{1}{E_1}(\sigma_{11} - \nu_1\sigma_{22}), \tag{5.4a}$$

$$\varepsilon_{22} = \frac{1}{E_2}(\sigma_{22} - \nu_2\sigma_{11}), \tag{5.4b}$$

$$\varepsilon_{12} = \frac{1}{2G_{12}}\sigma_{12}, \tag{5.4c}$$

$$\frac{\nu_1}{E_1} = \frac{\nu_2}{E_2}. \tag{5.4d}$$

The stress and moment resultants are related to F and w through the following expressions:

$$N_{11} = \frac{1}{a^2}\frac{\partial^2 F}{\partial x_2^2}, \tag{5.5a}$$

$$N_{22} = \frac{1}{a^2}\frac{\partial^2 F}{\partial x_1^2}, \tag{5.5b}$$

$$N_{12} = -\frac{1}{a^2}\frac{\partial^2 F}{\partial x_1 \partial x_2}, \tag{5.5c}$$

$$M_{11} = -\frac{D_1}{a^2}\left(\frac{\partial^2 w}{\partial x_1^2} + \nu_2\frac{\partial^2 w}{\partial x_2^2}\right), \tag{5.5d}$$

$$M_{22} = -\frac{D_2}{a^2}\left(\frac{\partial^2 w}{\partial x_2^2} + \nu_1\frac{\partial^2 w}{\partial x_1^2}\right), \tag{5.5e}$$

$$V_1 = Q_1 + \frac{\partial M_{12}}{\partial x_2} = -\frac{D_1}{a^3}\left[\frac{\partial^3 w}{\partial x_1^3} + \left(\nu_2 + \frac{h^3 G_{12}}{3D_1}\right)\frac{\partial^3 w}{\partial x_1 \partial x_2^2}\right], \tag{5.5f}$$

$$V_2 = Q_2 + \frac{\partial M_{12}}{\partial x_1} = -\frac{D_2}{a^3}\left[\frac{\partial^3 w}{\partial x_2^3} + \left(\nu_1 + \frac{h^3 G_{12}}{3D_2}\right)\frac{\partial^3 w}{\partial x_1^2 \partial x_2}\right], \tag{5.5g}$$

where

$$D_k = E_k h^3/12(1-\nu_1\nu_2)\ , \quad (k=1,2). \tag{5.6}$$

The membrane and bending stress components are obtained from relations of the form

$$\sigma_{11}^m = N_{11}/h, \ldots, \sigma_{11}^b = 12M_{11}Z/h^3, \ldots \tag{5.7}$$

In solving the problem, for example by expressing the functions F and w in terms of appropriate Fourier integrals, (2) may be reduced to a system of two fourth order linear ordinary differential equations. The characteristic function of this system will be an 8th degree polynomial the coefficients of which will be functions of the transform variable. For the problem to be analytically tractable, it is essential that the roots of the characteristic equation be obtainable in closed form. For anisotropic shells in general and for orthotropic shells in particular this does not seem to be possible. In order to express the roots in closed form the operators ∇_1^4 and ∇_2^4 must be properly factorized. From equations (5.3) it may be seen that these operators can indeed be factorized and expressed in the following form

$$\nabla_1^4 = \left[\frac{\partial^2}{\partial x_1^2} + \sqrt{(E_2/E_1)}\,\frac{\partial^2}{\partial x_2^2}\right] = \nabla_2^4 \tag{5.8}$$

if the elastic constants satisfy the following conditions:

$$[\nu_2 + 2(1-\nu_1\nu_2)G_{12}/E_1]\sqrt{(E_1/E_2)} = 1\ , \tag{5.9a}$$

$$\left(\frac{E_2}{2G_{12}} - \nu_2\right)\sqrt{(E_1/E_2)} = 1 \ . \tag{5.9b}$$

Now, by direct substitution it may easily be shown that the conditions (9) are satisfied provided the elastic constants are related by

$$G_{12} = \frac{\sqrt{(E_1E_2)}}{2[1+\sqrt{(\nu_1\nu_2)}]} . \tag{5.10}$$

Considering also the relation in equation (5.4d), this means that the sheet material has only three independent constants. Such a material is said to be "specially orthotropic". The analysis and certain results given in this chapter will then be valid only for those sheet materials in which the measured value of G_{12} and that calculated from equation (5.10) in terms of measured E_i and ν_i, $(i = 1,2)$ are in reasonably good agreement.

If the variables are changed once more as follows

$$x_1 = x \ , \ (E_1/E_2)^{1/4}x_2 = y \ , \tag{5.11}$$

the operators ∇_1^4 and ∇_2^4 become

$$\nabla_1^4 = \nabla_2^4 = \left[\frac{\partial^2}{\partial x^2} + \frac{\partial^2}{\partial y^2}\right]^2 = \nabla^4 \ . \tag{5.12}$$

With equation (5.12), equations (2) become identical to the differential equations for isotropic shells in which E and $D = Eh^3/[12(1-\nu^2)]$ are replaced by E_2 and D_1, respectively, i.e.,

$$D_1\nabla^4 w(x,y) - \frac{a^2}{R}\frac{\partial^2}{\partial x^2}F(x,y) = 0 \ , \tag{5.13a}$$

$$\nabla^4 F(x,y) + \frac{h^2E_2a^2}{R}\frac{\partial^2}{\partial x^2}w(x,y) = 0 \ . \tag{5.13b}$$

Let the stress and moment resultants on $y = 0$, $-a < X < a$ obtained from the solution of the shell under given external loads by ignoring the crack be

$$N_Y(X,0) = N_Y^o(X) = n_o(x) \ , \tag{5.14a}$$

$$N_{XY}(X,0) = N_{XY}^o(X) = t_o(x) \ , \tag{5.14b}$$

$$M_Y(X,0) = M_Y^o(X) = m_o(x) \ , \tag{5.14c}$$

$$V_Y(X,0) = V_Y^o(X) = v_o(x) \ . \tag{5.14d}$$

Considering the perturbation problem and referring to (5.1), (5.5), and (5.11), the system of differential equations (5.13) must then be solved under the following boundary conditions specified on the crack surface:

$$\lim_{y \to \mp 0} \frac{D}{a^2} \left[c^2 \frac{\partial^2 w}{\partial y^2} + \nu_1 \frac{\partial^2 w}{\partial x^2} \right] = m_o(x) \ , \tag{5.15a}$$

$$\lim_{y \to \mp 0} \frac{1}{a^2} \frac{\partial^2 F}{\partial x^2} = - n_o(x) \ , \tag{5.15b}$$

$$\lim_{y \to \mp 0} \frac{c}{a^2} \frac{\partial^2 F}{\partial x \partial y} = t_o(x) \ , \tag{5.15c}$$

$$\lim_{y \to \mp 0} \frac{D_2}{a^3} \left[c^3 \frac{\partial^3 w}{\partial y^3} + c \left(\nu_1 + \frac{h^3 G_{12}}{3 D_2} \right) \frac{\partial^3 w}{\partial^2 x \partial y} \right] = v_o(x) \ , \ (-1 < x < 1) \tag{5.15d}$$

where

$$c = (E_1/E_2)^{1/4} \ . \tag{5.16}$$

It is now clear that by properly decomposing the input functions given by equations (5.15) into even and odd components, the solution of the general problem may be expressed as the sum of a "symmetric" and a "skew-symmetric" solution. In the following two sections the solutions of these problems will be presented in some detail.

5.3 The Skew-Symmetric Problem

From a practical view point the important skew-symmetric problem is that having the following crack surface tractions:

$$m_o(x) = 0,\ n_o(x) = 0,\ t_o(x) = t_o(-x),\ v_o(x) = -v_o(-x),\ (-1<x<1). \qquad (5.17)$$

Outside the crack, the antisymmetry of the problem and the conditions of continuity require that

$$M_Y(X,0) = 0\ ,\ N_Y(X,0) = 0\ , \qquad (5.18a)$$

$$\lim_{y\to+0} \frac{\partial^n}{\partial y^n} w(x,y) = \lim_{y\to-0} \frac{\partial^n}{\partial y^n} w(x,y)\ ,\ (n=0,1,2,3)\ , \qquad (5.18b)$$

$$\lim_{y\to+0} \frac{\partial^n}{\partial y^n} F(x,y) = \lim_{y\to-0} \frac{\partial^n}{\partial y^n} F(x,y)\ ,\ (n=0,1,2,3)\ ,\ |x|>1\ . \qquad (5.18c)$$

Since the external loads in equations (5.17) are self-equilibrating local tractions, the functions F and w satisfy the regularity conditions at $x = \mp\infty$ and hence may be expressed in terms of Fourier integrals. Thus using the symmetry considerations, after some routine manipulations the solution of equations (5.13) may be expressed as

$$w(x,y) = \mathrm{sgn}(y) \int_0^\infty \sum_1^4 Q_j(\alpha) e^{m_j|y|} \sin\alpha x\ d\alpha\ , \qquad (5.19a)$$

$$F(x,y) = \mathrm{sgn}(y) \int_0^\infty \sum_1^4 K_j Q_j(\alpha) e^{m_j|y|} \sin\alpha x\ d\alpha\ , \qquad (5.19b)$$

where the functions $Q_j(\alpha)$, $(j=1,\ldots,4)$ are unknown and

$$K_1 = K_2 = -i(E_2 h D_1)^{\frac{1}{2}}\ ,\quad K_3 = K_4 = i(E_2 h D_1)^{\frac{1}{2}}\ ,$$

$$m_1 = -(\alpha^2 + i_1\lambda\alpha)^{\frac{1}{2}}\ ,\qquad m_2 = -(\alpha^2 - i_1\lambda\alpha)^{\frac{1}{2}}\ ,$$

$$m_3 = -(\alpha^2 + i_2\lambda\alpha)^{\frac{1}{2}}\ ,\qquad m_4 = -(\alpha^2 - i_2\lambda\alpha)^{\frac{1}{2}}\ ,$$

$$i_1 = e^{\pi i/4} \ , \ i_2 = e^{-\pi i/4} \ , \ \lambda^4 = 12(E_2/E_1)(1 - \nu_1\nu_2)\frac{a^4}{R^2h^2} \tag{5.20}$$

Substituting from equations (5.19) into equations (5.15a), (5.15b), (5.17a), (5.17b), and (5.18a) it is found that

$$Q_3 = \left[\frac{\alpha(\nu_1 - c^2)}{i_2\lambda c^2} + \frac{1}{2}\right](Q_1 + Q_2) - \frac{i}{2}(Q_1 - Q_2) \ , \tag{5.21a}$$

$$Q_4 = -\left[\frac{\alpha(\nu_1 - c^2)}{i_2\lambda c^2} - \frac{1}{2}\right](Q_1 + Q_2) + \frac{i}{2}(Q_1 - Q_2) \ . \tag{5.21b}$$

The two remaining equations to determine Q_j $(j = 1,..,4)$ are obtained from the mixed boundary conditions in equations (5.15c), (5.15d), (5.18c) and (5.18d). Since w and F are odd functions of y, equations (5.18c) and (5.18d) are automatically satisfied for $n = 1$ and $n = 3$. Using equations (5.21) and (5.19) it may be shown that the conditions in equations (5.18c) and (5.18d) for $n = 0$ and $n = 2$ will be satisfied if

$$\int_0^\infty (Q_1 + Q_2)\sin\alpha x \, d\alpha = 0 \ , \tag{5.22a}$$

$$\int_0^\infty (Q_1 + Q_2)\alpha^2\sin\alpha x \, d\alpha = 0 \ , \tag{5.22b}$$

$$\int_0^\infty \frac{\nu_1 - c^2}{c^2}(Q_1 + Q_2)\alpha^2\sin\alpha x \, d\alpha + \int_0^\infty i_1\lambda(Q_1 - Q_2)\alpha\sin\alpha x \, d\alpha = 0 \ , \ (|x| > 1) \ . \tag{5.22c}$$

Here equations (5.22a) and (5.22b) refer to the conditions that w and $\partial^2 w/\partial y^2$ vanish on $y = 0$, $|x| > 1$. Since analytically equation (5.22b) follows from equation (5.22a), equations (5.22) is actually equivalent to only two independent conditions. For dimensional consistency these conditions will be selected as follows:

$$\int_0^\infty (Q_1 + Q_2)\alpha^2 \sin\alpha x \, d\alpha = 0 \ , \tag{5.23a}$$

$$\int_0^\infty i_1\lambda(Q_1 - Q_2)\alpha \sin\alpha x \, d\alpha = 0 \ , \quad |x|>1 \ . \tag{5.23b}$$

With the selection of equation (5.23) as the conditions for $|x|>1$ it should be noted that a single-valuedness condition i.e., $w=0$ for $y=0$, $|x|>1$ still remains to be satisfied. This condition will be necessary to obtain a unique solution for the resulting integral equations.

Substituting from equations (5.19) into equation (5.15c) and (5.15d), and again, for dimensional consistency, integrating equation (5.15d), it is found that

$$\lim_{y\to+0} \left[-\frac{c}{a^2} \int_0^\infty \sum_1^4 K_j m_j Q_j e^{m_j y} \alpha \cos \alpha x \, d\alpha \right] = - t_0(x) \ , \tag{5.24a}$$

$$\lim_{y\to+0} \int_0^x \left\{ -\frac{D_2}{a^3} \int_0^\infty \sum_1^4 \left[c^3 m_j^3 - \alpha^2 c m_j \left(\nu_1 + \frac{h^3 G_{12}}{3D_2} \right) \right] Q_j e^{m_j y} \sin \alpha x \, d\alpha \right\} dx$$

$$= - \int_0^x v_0(x)dx \ , \ (|x|<1) \ . \tag{5.24b}$$

With equations (5.21), (5.23) and (5.24) give a system of dual integral equations to determine Q_1 and Q_2. Define now the following auxiliary functions:

$$u_1(x) = \int_0^\infty i_1\lambda\alpha(Q_1 - Q_2)\sin\alpha x \, d\alpha \ , \tag{5.25a}$$

$$u_2(x) = \int_0^\infty \alpha^2(Q_1 + Q_2)\sin\alpha x \, d\alpha \ , \quad 0 \leq x < \infty \ . \tag{5.25b}$$

Note that u_1 and u_2 are related to the second derivatives of w and F and hence are expected to have the same type of singularity as N_{ij} and M_{ij} at the crack tips ($x=\mp 1$, $y=0$). From equations (5.25) and (5.23) it follows that

$$Q_1 - Q_2 = \frac{2}{\pi i_1 \lambda \alpha} \int_0^1 u_1(t)\sin\alpha t \, dt \ , \tag{5.26a}$$

$$Q_1 + Q_2 = \frac{2}{\pi\alpha^2} \int_0^1 u_2(t)\sin\alpha t \, dt \ . \tag{5.26b}$$

Substituting now from equations (5.26) and (5.21) into equations (5.24) and observing that u_1 and u_2 are odd functions, the following integral equations are obtained to determine u_1 and u_2:

$$\lim_{y\to+0} \frac{1}{\pi} \int_{-1}^{1} \sum_{1}^{2} h_{ij}(x,t,y)u_j(t)dt = f_i(x) \ , \ (i = 1,2, \ |x|<1) \ , \tag{5.27}$$

where

$$f_1(x) \ \frac{ia^2 t_0(x)}{c\sqrt{(E_2 h D_1)}} \ , \ f_2(x) = \frac{a^3}{D_2} \int_0^x v_0(x)dx \ , \tag{5.28}$$

$$h_{1j}(x,t,y) = \int_0^\infty F_{1j}(\alpha,y)\sin\alpha(t-x)d\alpha \ , \ \ (j = 1,2) \ , \tag{5.29a}$$

$$F_{11}(\alpha,y) = \frac{1}{2}\left[-\frac{\alpha^2}{i_1\lambda} n_1 - \alpha n_2 - \frac{\alpha^2}{i_2\lambda} n_3 - \alpha n_4\right] \ , \tag{5.29b}$$

$$F_{12}(\alpha,y) = \frac{1}{2}\left[-i_1\lambda n_1 - \alpha n_2 + \left(\frac{2\alpha^2(\nu_1 - c^2)}{i_2\lambda c^2} + i_2\lambda\right) n_3 + \left[\frac{2\alpha(\nu_1 - c^2)}{c^2} + \alpha\right] n_4\right] \tag{5.29c}$$

$$h_{2j}(x,t,\alpha) = \int_0^\infty F_{2j}(\alpha,y)[\sin\alpha(t-x) - \sin\alpha t]d\alpha \ , \ \ (j = 1,2) \ , \tag{5.30a}$$

$$F_{21}(\alpha,y) = \frac{1}{2}\left[\left[c^2 - \nu_1 - \frac{h^3 G_{12}}{3D_2}\right]\left[\frac{\alpha^2}{i_1\lambda} n_1 - \frac{\alpha^2}{i_2\lambda} n_3\right] + \left[2c^2 - \nu_1 - \frac{h^3 G_{12}}{3D_2}\right] \alpha(n_2 - n_4) + i_1\lambda c^2 n_1 - i_2\lambda c^2 n_3\right] \ , \tag{5.30b}$$

$$F_{22}(\alpha,y) = \frac{1}{2}\left[\left[c^2 - \nu_1 - \frac{h^3 G_{12}}{3D_2}\right]\left[\alpha n_2 + \frac{2\alpha^2(\nu_1 - c^2)}{i_2\lambda c^2} n_3 + \alpha n_4\right] + \left[2c^2 - \nu_1 - \frac{h^3 G_{12}}{3D_2}\right] \left[i_1\lambda n_1 + \frac{2\alpha(\nu_1 - c^2)}{c^2} n_4 + i_2\lambda n_3\right]\right.$$

$$+ \frac{i\lambda^2 c^2}{\alpha} n_2 + 2i_2\lambda(\nu_1 - c^2)n_3 - \frac{i\lambda^2 c^2}{\alpha} n_4 \Big] . \qquad (5.30c)$$

$$n_1 = \frac{e^{m_1 y}}{m_1} - \frac{e^{m_2 y}}{m_2} , \quad n_2 = \frac{e^{m_1 y}}{m_1} + \frac{e^{m_2 y}}{m_2} ,$$

$$n_3 = \frac{e^{m_3 y}}{m_3} - \frac{e^{m_4 y}}{m_4} , \quad n_4 = \frac{e^{m_3 y}}{m_3} + \frac{e^{m_4 y}}{m_4} , \qquad (5.31)$$

By examining the asymptotic behavior of the integrands for large and small values of α in equations (5.29) and (5.30) for the kernels h_{ij}, it may be seen that some of the integrals are uniformly convergent. In these integrals the limit can be put under the integral sign and the resulting kernels are simple Fredholm kernels. In the expression $\sin\alpha p$ ($p = t - x$ or $p = t$) as $p \to 0$ it may also be seen that the remaining integrals become divergent, meaning that the kernels contain singularities. These singular parts of the kernels may be separated in a standard way by adding and subtracting the asymptotic value of the integrand for large values of α. For example, noting that for large α

$$\alpha^2 n_1(\alpha,y) = i_1\lambda e^{-\alpha y} + e^{-\alpha y}\, 0(\alpha^{-2}) , \quad y > 0 , \qquad (5.32)$$

it is seen that

$$\int_0^\infty \alpha^2 n_1(\alpha,y)\sin\alpha p \, d\alpha = i_1\lambda \int_0^\infty e^{-\alpha y}\sin\alpha p \, d\alpha + \int_0^\infty [\alpha^2 n_1(\alpha,y) - i_1\lambda e^{-\alpha y}]\sin\alpha p \, d\alpha$$

$$= i_1\lambda \frac{p}{p^2+y^2} + \int^\infty \left[\left(\frac{e^{m_1 y}}{m_1} - \frac{e^{m_2 y}}{m_2} \right) \alpha^2 - i_1\lambda e^{-\alpha y} \right] \sin\alpha p \, d\alpha \qquad (5.33)$$

where the last integral is uniformly convergent for all p and $y \to 0$, and hence, the limit $y = 0$ can be put under the integral sign, whereas the integrated term gives a Cauchy type singularity $1/p$. Similarly

$$\int_0^\infty \alpha n_2(\alpha,y)\sin\alpha p \, d\alpha = \frac{2p}{p^2+y^2} + \int_0^\infty \left[\left(\frac{e^{m_1 y}}{m_1} + \frac{e^{m_2 y}}{m_2} \right) \alpha - 2e^{-\alpha y} \right] \sin\alpha p \, d\alpha . \qquad (5.34)$$

Thus, after separating the singular parts of the kernels and goint to limit, equation (5.27) becomes

$$\int_{-1}^{1} \sum_{1}^{2} a_{ij}u_j(t)\,\frac{dt}{t-x} + \int_{-1}^{1} \sum_{1}^{2} k_{ij}(x,t)u_j(t)dt = \pi f_i(x) \quad (|x|<1)\,, \tag{5.35}$$

where

$$\begin{aligned} &a_{11} = 1, \quad a_{12} = 1 - \frac{\nu_1}{c^2}\,, \quad a_{21} = 0, \\ &a_{22} = -3\nu_1 + c^2 + \left[1 + \frac{\nu_1}{c^2}\right]\left[\nu_1 + \frac{h^3 G_{12}}{3D_2}\right]\,, \end{aligned} \tag{5.36}$$

and the Fredholm kernels $k_{ij}(x,t)$ are given by

$$k_{1j}(x,t) = \int_0^\infty [F_{1j}(\alpha,0) - a_{1j}]\sin\alpha(t-x)d\alpha\,, \quad (j=1,2)\,, \tag{5.37}$$

and

$$k_{21}(x,t) = \int_0^\infty F_{21}(\alpha,0)[\sin\alpha(t-x) - \sin\alpha t]d\alpha\,, \tag{5.38a}$$

$$k_{22}(x,t) = -\frac{a_{22}}{t} + \int_0^\infty [F_{22}(\alpha,0) - a_{22}]\sin\alpha(t-x) - \sin\alpha t]d\alpha\,. \tag{5.38b}$$

Since u_1 and u_2 are related to the second derivatives of F and w, the elements of the fundamental matrix of the singular integral equations (5.35) will be $(1-x^2)^{-\frac{1}{2}}$ and the solution will be of the form

$$u_j(x) = G_j(x)(1-x^2)^{-\frac{1}{2}}\,, \quad (j=1,2)\,, \quad (|x|<1) \tag{5.39}$$

where the functions G_j are bounded in $(-1\leq x\leq 1)$. Thus the index of the system in equation (5.35) is $\kappa = 1$, and hence theoretically the solution is not unique and will contain two arbitrary constants [22]. These constants are determined by using the single-valuedness condition mentioned earlier, namely that $w(x,0) = 0$ for $|x|>1$. Referring to equations (5.19), (5.21), (5.22) and (5.25) it may be shown that $2u_2(x) = -(\partial^2/\partial x^2)w(x,0)$. Since $u_2(x) = 0$ for $|x|>1$, it

then follows that for $w(x,0)$ for $|x|>1$ $u_2(x)$ must satisfy the following conditions

$$\int_{-1}^{1} u_2(x)dx = 0 \ , \quad \int_{-1}^{1} dx \int_{-1}^{x} u_2(t)dt = 0 \ . \tag{5.40}$$

The unknown functions G_1 and G_2 defined by equation (5.39) may be obtained from equations (5.35) and (5.40) in a straightforward way by using the technique outlined in [23].

To examine the asymptotic behavior of the stresses around the crack tips let us assume that the bounded functions G_1 and G_2 are expressed in terms of the following infinite series:

$$G_1(x) = \sum_{1}^{\infty} A_n T_{2n-1}(x) \ , \quad G_2(x) = \sum_{1}^{\infty} B_n T_{2n-1}(x) \ , \tag{5.41}$$

where $T_k(x)$ is the Chebyshev polynomial of the first kind and the symmetry property of $u_j(x) = - u_j(-x)$ $(j = 1,2)$ has been used. From equations (5.26), (5.39) and (5.41) by using the relation [24]

$$\int_{0}^{1} T_{2n+1}(x)(1 - x^2)^{-1/2} \sin\alpha x \ d\alpha = (-1)^n \frac{\pi}{2} J_{2n+1}(\alpha) \ , \ (n = 0,1,2\ldots) \tag{5.42}$$

it may be shown that

$$i_1 \lambda\alpha(Q_1 - Q_2) = \sum_{1}^{\infty}(-1)^{n-1} A_n J_{2n-1}(\alpha) \ , \tag{5.43a}$$

$$\alpha^2(Q_1 + Q_2) = \sum_{1}^{\infty}(-1)^{n-1} B_n J_{2n-1}(\alpha) \ . \tag{5.43b}$$

The expressions for the stresses may then be obtained by substituting from equations (5.43), (5.21), (5.19) into (5.5) and (5.7). For example,

$$\sigma_{xy}^{m} = - \frac{c}{ha^2} \frac{\partial^2 F}{\partial x \partial y} = \frac{c}{ha^2} \int_{0}^{\infty} \sum_{1}^{4} K_j Q_j(\alpha) m_j \alpha e^{m_j y} \cos\alpha x \ d\alpha \ , \quad (y \geq 0) \ . \tag{5.44}$$

At $(y = 0, \ x = \mp 1)$, the integrals in (5.44) are divergent, meaning that the

stresses will have a singularity at the crack tips. Noting that the integrand in equation (5.44) is integrable around $\alpha = 0$ and is bounded and continuous elsewhere in the domain, the divergent behavior of the integral must be due to the asymptotic behavior of the integrand for large values of α. Thus, substituting from equation (5.43) and (5.21), equation (5.44) may be expressed as

$$\sigma^m_{xy} = \frac{c}{ha^2}\, i(E_2 h D_1)^{\frac{1}{2}} \sum_1^\infty (-1)^{n-1}\left[A_n - \frac{\nu_1 - c^2}{c^2} B_n\right]$$

$$x \int_0^\infty J_{2n-1}(\alpha)[-1 + \alpha y + 0(\alpha^{-1})]e^{-\alpha y}\cos\alpha x \, d\alpha \quad (y \geq 0) \, . \tag{5.45}$$

Noting that for large values of α [24]

$$J_{2n-1}(\alpha) \cong (-1)^{n-1} J_1(\alpha) \cong \left(\frac{2}{\pi\alpha}\right)^{\frac{1}{2}} (-1)^{n-1}\left[\cos\left(\alpha - \frac{3\pi}{4}\right) + 0(\alpha^{-1})\right] (n = 1,2,\ldots), \tag{5.46}$$

and using the results in [24] to evaluate the integrals, we obtain the leading term in (5.45) as follows:

$$\sigma^m_{xy}(r,\theta) = \frac{ci}{ha^2}\, (E_2 h D_1)^{\frac{1}{2}} \sum_1^\infty \left[- A_n + \frac{\nu_1 - c^2}{c^2} B_n\right]$$

$$x \frac{1}{4\sqrt{(2r)}} \left[3\cos\frac{\theta}{2} + \cos\frac{5\theta}{2}\right] + 0(r^{\frac{1}{2}}) \, , \tag{5.47}$$

where (r,θ) are the polar coordinates measured from the crack tip,

$$(x = 1, y = 0) \, , \quad r^2 = (x-1)^2 + y^2 \, , \quad \tan\theta = y/(x-1) \, .$$

For example, if

$$t_0(x) = N_0 \, , \quad v_0(x) = 0 \, ,$$

defining the following normalized functions (see equation (5.28)):

$$G_j^*(x) = G_j(x)/u_o \ , \quad (j=1,2) \ , \tag{5.48a}$$

$$u_o = \frac{a^2 N_o}{c\sqrt{(E_2 h D_1)}} = \frac{\lambda^2 R N_o c}{h\sqrt{(E_1 E_2)}} \ , \tag{5.48b}$$

$$G_1^*(x) = \sum_1^\infty a_n T_{2n-1}(x) \ , \tag{5.48c}$$

$$G_2^*(x) = \sum_1^\infty b_n T_{2n-1}(x) \ , \tag{5.48d}$$

equation (5.46) may be expressed as

$$\sigma_{xy}^m = \left(\frac{N_o\sqrt{a}}{h}\right)\left[i\sum_1^\infty\left(-a_n + \frac{\nu_1 - c^2}{c^2} b_n\right)\right]\frac{1}{4\sqrt{(2ra)}}\left(3\cos\frac{\theta}{2} + \cos\frac{5\theta}{2}\right) + O(r^{\frac{1}{2}}) \tag{5.49}$$

Observing that the stress intensity factor in a flat plate under uniform shear stress N_o/h and that in a shell are defined by

$$k_p = N_o\sqrt{(a)/h} \ , \quad k_s^m = \lim_{x\to 1}\sqrt{2(x-1)a}\ \sigma_{xy}^m(x,0) \ , \tag{5.50}$$

from equation (5.49) the membrane component of the stress intensity factor ratio for the shell is found to be

$$C_m = \frac{k_s^m}{k_p} = i\sum_1^\infty\left(-a_n + \frac{\nu_1 - c^2}{c^2} b_n\right) . \tag{5.51}$$

Further, noting that $T_n(1) = 1$, $(n = 0,1,2,\ldots)$ from equation (5.48) and (5.50) it follows that

$$C_m = \frac{k_s^m}{k_p} = \left[-G_1^*(1) + \frac{\nu_1 - c^2}{c^2} G_2^*(1)\right] i \ . \tag{5.52}$$

The remaining membrane stresses may be obtained in a similar way. Thus, for small values of r the membrane stresses in the shell may be expressed as

$$\sigma^m_{xx}(r,\theta) = \frac{C_m k_p}{4c\sqrt{(2ra)}}\left[7\sin\frac{\theta}{2} + \sin\frac{5\theta}{2}\right] + O(r^{\frac{1}{2}}) \ , \tag{5.53a}$$

$$\sigma^m_{yy}(r,\theta) = \frac{C_m k_p}{4\sqrt{(2ra)}}\left[-\sin\frac{\theta}{2} + \sin\frac{5\theta}{2}\right] + O(r^{\frac{1}{2}}) \ , \tag{5.53b}$$

$$\sigma^m_{xy}(r,\theta) = \frac{C_m k_p}{4\sqrt{(2ra)}}\left[3\cos\frac{\theta}{2} + \cos\frac{5\theta}{2}\right] + O(r^{\frac{1}{2}}) \ . \tag{5.53c}$$

Defining now the bending component of the stress intensity factor by

$$k^b_s = \lim_{x\to 1}\sqrt{2(x-1)a}\ \ \sigma^b_{xy}(x,0,h) = C_b k_p \ ; \tag{5.54}$$

in a similar way the asymptotic expressions for the bending stresses around the crack tip may be obtained as follows:

$$\sigma^b_{xy}(r,\theta,Z) = \frac{C_b k_p}{\sqrt{(2ra)}}\frac{2Z}{h}\frac{1}{4[2+(\nu_1-c^2)/c^2]}\left[\left\{8 + \frac{3(\nu_1 - c^2)}{c^2}\cos\frac{\theta}{2}\right.\right.$$
$$\left.\left. + \frac{\nu_1 - c^2}{c^2}\cos\frac{5\theta}{2}\right\] + O(r^{\frac{1}{2}}) \ , \tag{5.55a}$$

$$\sigma^b_{xx}(r,\theta,Z) = \frac{C_b k_p}{\sqrt{(2ra)}}\frac{2Z}{h}\frac{c}{4[2+(\nu_1-c^2)/c^2][1-\sqrt{(\nu_1\nu_2)}]}$$
$$\times\left\{\left[8(1-\nu_2c^2) - \frac{\nu_1 - c^2}{c^2}(1+7\nu_2c^2)\right]\sin\frac{\theta}{2}\right.$$
$$\left. + \frac{\nu_1 - c^2}{c^2}(1-\nu_2c^2)\sin\frac{5\theta}{2}\right\} + O(r^{\frac{1}{2}}) \ , \tag{5.55b}$$

$$\sigma^b_{yy}(r,\theta,Z) = \frac{C_n k_p}{\sqrt{(2ra)}}\frac{2Z}{h}\frac{c^2-\nu_1}{4[2+(\nu_1-c^2)/c^2][1-\sqrt{(\nu_1\nu_2)}]c^3}$$
$$\times\left[\left(\frac{\nu_1 - c^2}{c^2} + 8c^2 - 8\right)\sin\frac{\theta}{2} - \frac{\nu_1 - c^2}{c^2}\sin\frac{5\theta}{2}\right] + O(r^{\frac{1}{2}}) \ , \tag{5.55c}$$

where the bending component of the stress intensity ratio is found to be:*

$$C_b = -\frac{\{3[1-\sqrt{(\nu_1\nu_2)}]\}^{\frac{1}{2}}}{1+\sqrt{(\nu_1\nu_2)}}\left(2+\frac{\nu_1-c^2}{c^2}\right) G_2^*(1) \ . \tag{5.56}$$

Thus, once the singular integral equations (5.35) are solved after normalization described by equations (5.48), the stress intensity factors can be obtained without further analysis. The analysis in this section remains valid for the isotropic shell with $E_1 = E_2 = E$, $\nu_1 = \nu_2 = \nu$, $G_{12} = G$, and $c = (E_1/E_2)^{\frac{1}{4}} = 1$.

5.4 The symmetric Problem

Consider now the symmetric problem in which the only external loads are the following crack surface tractions (see equations (5.14)):

$$m_0(x) = m_0(-x) \ , \quad n_0(x) = n_0(-x) \ , \quad t_0(x) = 0$$

$$v_0(x) = 0 \ , \quad (-1<x<1) \tag{5.57}$$

In addition to the boundary conditions specified by equations (5.14), (5.15), and (5.57) on the crack surface ($-1<x<1$, $y=0$), outside the crack ($|x|>1$, $y=0$) the symmetry and continuity considerations require that (18c,d) and the following conditions be satisfied:

$$N_{XY}(X,0) = n_{xy}(x,0) = 0 \ , \quad V_Y(X,0) = v_y(x,0) = 0 \quad (|x|>1) \ . \tag{5.58}$$

In this case, using again the Fourier transforms, the solution of equation (5.13) may be expressed as

$$w(x,y) = \int_0^\infty \sum_1^4 R_j(\alpha) e^{m_j|y|} \cos\alpha x \, d\alpha \ , \tag{5.59a}$$

*See [16] for details.

$$F(x,y) = \int_0^\infty \sum_1^4 K_j R_j(\alpha) e^{m_j|y|} \cos\alpha x \, d\alpha \ , \tag{5.59b}$$

where K_j and m_j are defined by equations (5.20). Substituting from equations (5.59) into (5.15), the homogeneous conditions in equations (5.57c), (5.57d), and (5.58) give the following two algebraic relations:

$$m_3 R_3 = \left(\frac{c_0\alpha}{i_2\lambda c^2} + \frac{1}{2}\right)(m_1 R_1 + m_2 R_2) + \frac{i}{2}(m_2 R_2 - m_1 R_1) \ , \tag{5.60a}$$

$$m_4 R_4 = \left(\frac{1}{2} - \frac{c_0\alpha}{i_2\lambda c^2}\right)(m_1 R_1 + m_2 R_2) - \frac{i}{2}(m_2 R_2 - m_1 R_1) \ , \tag{5.60b}$$

$$c_0 = \nu_1 + c^2[1 - 2\sqrt{(\nu_1\nu_2)}] \ , \tag{5.60c}$$

After some manipulations it can be shown that the continuity conditions are satisfied if

$$\int_0^\infty (m_1 R_1 + m_2 R_2)\cos\alpha x \, d\alpha = 0 \ , \tag{5.61a}$$

$$\int_0^\infty \frac{i_1\lambda}{\alpha}(m_1 R_1 - m_2 R_2)\cos\alpha x \, d\alpha = 0 \ , \quad (|x|>1) \ . \tag{5.61b}$$

The remaining boundary conditions in equations (5.57a), (5.57b) with (5.14), (5.15), and (5.59) may be expressed as

$$\lim_{y\to+0} \int_0^x \left[-\frac{1}{a^2}\int_0^\infty \sum_1^4 (c^2 m_j^2 - \nu_1\alpha^2) R_j e^{m_j y}\cos\alpha x \, d\alpha\right]dx = -\frac{1}{D_2}\int_0^x m_0(x)dx \ , \tag{5.62a}$$

$$\lim_{y\to+0} \int_0^x \left[\frac{1}{a^2}\int_0^\infty \sum_1^4 K_j R_j e^{m_j y}\alpha^2\cos\alpha x \, d\alpha\right]dx = -\int_0^x n_0(x)dx \ , \ (-1<x<1) \ . \tag{5.62b}$$

With equations (5.6), (5.61) and (5.62) give a system of dual integral equations to determine R_1 and R_2. In equation (5.62) the integral equations are written in integrated form to make them dimensionally consistent with equations (5.61) (i.e., the quantities which appear in equations (5.61) and (5.62) now represent the first derivatives of F and w). Defining

$$\int_0^\infty (m_1R_1 + m_2R_2)\cos\alpha x \, d\alpha = v_1(x) \ , \tag{5.63a}$$

$$\int_0^\infty \frac{i_1\lambda}{\alpha} (m_1R_1 - m_2R_2)\cos\alpha d\alpha = v_2(x) \ , \quad 0\leq x<\infty \tag{5.63b}$$

and using equation (5.60), and the symmetry conditions $v_j(x) = v_j(-x)$, $(j=1,2)$, equations (5.61) and (5.62) may be reduced to:

$$\lim_{y\to+0} \frac{1}{\pi} \int_{-1}^{1} \sum_{1}^{2} g_{ij}(x,t,y)v_j(t)dt = p_i(x) \ , \ (i=1,2) \ , \ (|x|<1) \ . \tag{5.64}$$

Following a procedure similar to that of the previous section to separate the singular kernels and going to limit, equation (5.64) may be put into the following standard form:

$$\int_{-1}^{1} \sum_{1}^{2} [\frac{b_{ij}}{t-x} + \ell_{ij}(x,t)]v_j(t)dt = \pi p_i(x) \ , \ (i=1,2, \ |x|<1) \tag{5.65}$$

where

$$p_1(x) = \frac{a^2}{i\sqrt{(E_2hD_1)}} \int_0^x n_0(x)dx \ , \ p_2(x) = \frac{a^2}{D_2} \int_0^x m_0(x)dx; \tag{5.66}$$

$$b_{11} = -\frac{2c_0}{c^2} \ , \ b_{12} = 2 \ , \ b_{21} = 4(c^2-\nu_1) + \frac{2c_0}{c^2}(2 + \nu_1 - c^2) \ ,$$

$$b_{22} = 2\lambda c^2(1 - i_2); \tag{5.67}$$

$$\ell_{11}(x,t) = \int_0^\infty [(\frac{\alpha}{m_1} + \frac{\alpha}{m_2} + 2) - \frac{2c_0}{i_2\lambda c^2}(\frac{\alpha^2}{m_3} - \frac{\alpha^2}{m_4} - i_2\lambda)$$

$$- (\frac{\alpha}{m_3} + \frac{\alpha}{m_4} + 2)]\sin\alpha(t-x)d\alpha \ , \tag{5.68a}$$

$$\ell_{12}(x,t) = \int_0^\infty [\frac{\alpha^2}{i_1\lambda}(\frac{1}{m_1} - \frac{1}{m_2}) + \frac{\alpha^2}{i_2\lambda}(\frac{1}{m_3} - \frac{1}{m_4}) - 2]\sin\alpha(t-x)d\alpha \ , \tag{5.68b}$$

$$\ell_{21}(x,t) = \int_0^\infty [(\nu_1 - c^2)(\frac{\alpha}{m_1} + \frac{\alpha}{m_2} + \frac{\alpha}{m_3} + \frac{\alpha}{m_4} + 4) - i_1\lambda c\ (\frac{1}{m_1} + \frac{1}{m_2})$$

$$- i_2\lambda c\ (\frac{1}{m_3} + \frac{1}{m_4}) - (c^2 - \nu_1)\ \frac{2c_0}{i_2\lambda c}\ (\frac{\alpha^2}{m_3} - \frac{\alpha^2}{m_4} - i_2\lambda)]\sin\alpha(t-x)d\alpha\ , \tag{5.68c}$$

$$\ell_{22}(x,t) = \int_0^\infty [\frac{\nu_1 - c^2}{i_1\lambda}\ (\frac{\alpha^2}{m_1} - \frac{\alpha^2}{m_2} - i_1\lambda) - \lambda c^2(\frac{\alpha}{m_1} + \frac{\alpha}{m_2} + 2)$$

$$+ \frac{c^2 - \nu_1}{i_2\lambda}\ (\frac{\alpha^2}{m_3} - \frac{\alpha^2}{m_4} - i_2\lambda) + i_2\lambda c^2(\frac{\alpha}{m_3} + \frac{\alpha}{m_4} + 2)]\sin\alpha(t-x)d\alpha\ . \tag{5.68d}$$

Here m_j and constants i_1, i_2, and λ are defined by equations (5.20) and c_0 is given by equation (5.60c).

From equations (5.63) and (5.59) it may be seen that physically the quantities v_1 and v_2 correspond to the first derivatives of F and w. Therefore, the elements of the fundamental matrix of the system of singular integral equations (5.65) will be $(1 - x^2)^{\frac{1}{2}}$ and the solution will be of the following form:

$$v_j(x) = H_j(x)(1 - x^2)^{\frac{1}{2}}\ ,\ (j = 1,2,\ |x|<1)\ , \tag{5.69}$$

where H_j is bounded in $-1 \leq x \leq 1$. Thus the index of the system in equations (5.65) is $\kappa = -1$, and there are no additional conditions (other than the consistency conditions of the singular integral equations) necessary for a unique solution [22]. Note, again, that equations (5.65) are complex and are equivalent to four real integral equations which may be solved numerically in a simple way by using the technique outlined in [23].

To examine the stress state around the crack tips let the functions H_j be expressed in terms of the following infinite series:

$$H_1(x) = \sum_0^\infty A_n U_{2n}(x)\ ,\ H_2(x) = \sum_0^\infty B_n U_{2n}(x)\ , \tag{5.70}$$

where $U_k(x)$ is the Chebyshev polynomial of the second kind and the symmetry property $v_j(x) = v_j(-x)$ has been used. By using the relation [24]

$$\int_0^1 U_{2n}(t)\sqrt{(1-t^2)}\cos\alpha t\, dt = (-1)^n \frac{\pi}{2}(2n+1)\frac{1}{\alpha}J_{2n+1}(\alpha) ,$$

$$(n = 0,1,2,..) , \tag{5.71}$$

from equations (5.63), (5.69), and (5.70) it follows that

$$m_1R_1 + m_2R_2 = \sum_0^\infty (-1)^n(2n+1)A_n \frac{1}{\alpha}J_{2n+1}(\alpha) , \tag{5.72a}$$

$$m_1R_1 - m_2R_2 = \frac{1}{i_1\lambda}\sum_0^\infty (-i)^n(2n+1)B_nJ_{2n+1}(\alpha) . \tag{5.72b}$$

Substituting into the stress expressions from equations (5.72), (5.60), and (5.59) and omitting the details it may now be shown that*

$$\sigma^m_{yy}(r,\theta) = \frac{i\sqrt{(E_2hD_1)}}{4ha^2}\sum_0^\infty (2n+1)\left(\frac{c_0}{c^2}A_n - B_n\right)x$$

$$x\,\frac{1}{\sqrt{2r}}\left(5\cos\frac{\theta}{2} - \cos\frac{5\theta}{2}\right) + O(r^{\frac{1}{2}}) \tag{5.73}$$

where (r,θ) are the polar coordinates at the crack tip defined by

$$r^2 = (x-1)^2 + y^2 , \quad \tan\theta = y/(x-1) .$$

Defining the membrane component of the stress intensity factor in the shell by

$$k^m_s = \lim_{x\to 1}\sqrt{2(x-1)a}\;\; \sigma^m_{yy}(x,0) , \tag{5.74}$$

and observing that $U_{2n}(1) = 2n+1$, k^m_s is found to be

$$k^m_s = \frac{i\sqrt{(E_2hD_1a)}}{ha^2}\left[\frac{c_0}{c^2}H_1(1) - H_2(1)\right] . \tag{5.75}$$

*See [16] for the evaluation of the related integrals.

For example, if $n_o(x) = N_o$ = constant, $m_o(x) = 0$, and the corresponding plate stress intensity factor is defined by $k_p = (N_o\sqrt{a})/h$, the membrane component of the stress intensity factor ratio becomes

$$A_m = \frac{k_s^m}{k_p} = i\left[\frac{c_o}{c^2} H_1^*(1) - H_2^*(1)\right] \tag{5.76}$$

where

$$H_j^*(x) = H_j(x) \frac{\sqrt{(E_2 h D_1)}}{N_o a^2}, \quad (j = 1,2) \tag{5.77}$$

the functions H_j^* are obtained from equations (5.65) after the normalization given by equation (5.77)

The reamining stress components may be obtained in a similar way. The asymptotic stress state in the neighborhood of the crack tip may then be expressed as

$$\sigma_{yy}^m(r,\theta) = A_m \frac{k_p}{\sqrt{(2ra)}} \frac{1}{4} \left(5\cos\frac{\theta}{2} - \cos\frac{5\theta}{2}\right) + O(r^{\frac{1}{2}}), \tag{5.78a}$$

$$\sigma_{xx}^m(r,\theta) = A_m \frac{k_p}{\sqrt{(2ra)}} \frac{c^2}{4} \left(3\cos\frac{\theta}{2} + \cos\frac{5\theta}{2}\right) + O(r^{\frac{1}{2}}), \tag{5.78b}$$

$$\sigma_{xy}^m(r,\theta) = A_m \frac{k_p}{\sqrt{(2ra)}} \frac{c}{4} \left(\sin\frac{\theta}{2} - \sin\frac{5\theta}{2}\right) + O(r^{\frac{1}{2}}), \tag{5.78c}$$

$$\sigma_{yy}^b(r,\theta, Z) = A_b \frac{k_p}{\sqrt{(2ra)}} \frac{Z}{2h} \left[\left(8\nu_o - 8\nu_c + \frac{5\nu_c\nu_o}{c^2}\right)\cos\frac{\theta}{2} - \frac{\nu_o\nu_c}{c^2}\cos\frac{5\theta}{2}\right] + O(r^{\frac{1}{2}}), \tag{5.79a}$$

$$\sigma_{xx}^b(r,\theta, Z) = A_b \frac{k_p}{\sqrt{(2ra)}} \frac{2Z}{h} \left[\left(8 + \frac{5\nu_c}{c^2} - 8\nu_c c^2 + 3\nu_2\nu_c\right)\cos\frac{\theta}{2} - \frac{\nu_c}{4c^2}(1 - \nu_2 c^2)\cos\frac{5\theta}{2}\right] + O(r^{\frac{1}{2}}), \tag{5.79b}$$

$$\sigma_{xy}^b(r,\theta,Z) = A_b \frac{k_p}{\sqrt{(2ra)}} \frac{Z}{h} \frac{a^2 h^3 G_{12}}{12 D_1} \left[\frac{\nu_c}{c^2}\sin\frac{5\theta}{2} - \left(8 + \frac{\nu_c}{c^2}\right)\sin\frac{\theta}{2}\right] + O(r^{\frac{1}{2}}), \tag{5.79c}$$

where

$$v_0 = c^2 - \nu_1,\ c = (E_1/E_2)^{\frac{1}{4}},\ \nu_c = c^2 - \left(\nu_1 + \frac{h^3 G_{12}}{3D_2}\right). \tag{5.80}$$

and the bending component of the stress intensity ratio is found to be

$$A_b = k_s^b/k_p = \frac{1}{k_p}\lim_{x\to 1}\sqrt{2(x-1)a}\ \sigma_{yy}^b(x,0,h)$$

$$= \frac{1}{2c^2}\frac{\sqrt{[12(1-\nu_1\nu_2)]}}{1-\nu_1\nu_2}\left[\frac{c_0}{c^2} - 2)(c^2-\nu_1) + 2c_0\right]H_1^*(1). \tag{5.81}$$

By letting $E_1 = E_2 = E$, $\nu_1 = \nu_2 = \nu$, $G_{12} = G$, and $c = 1$ the results of this section too reduce to the solution of isotropic cylindrical shell.

The "bulging" of the shell in the neighborhood of the crack, i.e., w may be directly evaluated in terms of the solution given in this section. Also, in the present as well in the two other ideal shell geometries (that is, in the cylindrical shell with an axial or a circumferential crack, and in the spherical shell with a meridional crack) it can be shown that the auxiliary functions defined to reduce the problem to singular integral equations are directly related to the crack surface displacements. For the isotropic shells these displacements are obtained and presented for various values of the shell parameter λ in [8].

The θ-dependence in the asymptotic stress expressions given by equations (5.53), (5.55), (5.78), and (5.79) is identical to the expressions for isotropic shells. However, note that the dimensionless coordinates r, θ, x, and y in the specially orthotropic shells are defined by

$$r^2 = (x-1)^2 + y^2,\ \tan\theta = y/(x-1),\ x = X/a,\ y = c/Ya. \tag{5.82}$$

where X, Y, Z are the actual rectangular coordinates and the actual geometric angle Θ in the shell is given by

$$\tan \Theta = Y/(X - a) = \frac{y}{c(x - 1)} = \frac{1}{c} \tan\theta \,. \tag{5.83}$$

Therefore, because of equation (5.83), the angular variation of the asymptotic stresses in the specially orthotropic shells is different and a good deal more complicated than that in isotropic shells.

The analysis given in this and the previous sections indicates that, since the roots of the characteristic equation m_j, $(j = 1,..,4)$, shown in equations (5.19) and (5.20) are functions of the transform variable α, $(0<\alpha<\infty)$, mathematically the problem would have been intractable if $m_j(\alpha)$ were not evaluated in closed form. This is essential for extracting the singular parts of the kernels of the resulting integral equations as well as for studying and obtaining the correct singular behavior of the solution. The analysis also shows that this critical aspect of the problem relating to the singular nature of the integral equations and their solution is entirely dependent on the asymptotic behavior of certain functions for large values of α (see, for example, equations (5.29) to (5.34)). The variable α appears in these functions explicitly as well as through $m_j(\alpha)$. In the equation which determines m_j, the coefficients of the characteristic function, which is an 8th degree polynomial, are functions of α. Therefore, for the problems in which the roots $m_j(\alpha)$ cannot be expressed in closed form, it appears that if the asymptotic solution of the characteristic equation giving $m_j(\alpha)$ for large values of α can be obtained correctly in closed form, then the singular parts of the kernels can be separated and the singular nature of the solution can be studied. Furthermore, by also evaluating

$m_j(\alpha)$ for small values of α in closed form and for intermediate discreet values of α numerically, at least in principle, it is possible to evaluate the Fredholm kernels in the integral equations numerically and, at the cost of a rather high computational effort, to obtain a meaningful approximate solution.

5.5 Results for a Specially Orthotropic Cylindrical Shell

In order to give an idea about the effect the material orthotropy may have on the stress intensity factors in a cylindrical shell containing a longitudinal through crack, in this section some numerical results on cylinders made of three different materials will be presented. These are an isotropic cylinder, a titanium cylinder which is mildly orthotropic, and a graphite cylinder which is strongly orthotropic. The measured elastic constants of the orthotropic materials are shown in Table 5.1. The table also shows the "average shear

Table 5.1 Elastic constants of the orthotropic materials

	Titanium	Graphite
E_1(psi)	1.507×10^7	1.5×10^6
E_2(psi)	2.08×10^7	40×10^6
ν_1	0.1966	0.0075
ν_2	0.2714	0.2000
G_{12}	6.78×10^6	4.0×10^6
$G_{av.}$	7.15×10^6	3.73×10^6

modulus" calculated from (see equation (5.10))

$$G_{av.} = \frac{\sqrt{(E_1 E_2)}}{2[1 + \sqrt{(\nu_1 \nu_2)}]}, \tag{5.84}$$

where E_1 is the modulus in the axial direction and the notation is given by

equations (5.4). If the measured shear modulus G_{12} were equal to the calculated modulus $G_{av.}$, then the material would be specially orthotropic and the analysis given in the previous sections would be valid without any approximations. The table indicates that these two values are sufficiently close so that the special orthotropy assumption may be used to study the effect of material orthotropy on the stress intensity factors.

Figures 5.2 to 5.5 show the results for a pressurized shell with an axial crack. The membrane and bending components of the stress intensity factor ratio A_m and A_b shown in the figures are defined by equations (5.74), (5.76) and (5.81). For the pressurized shell the corresponding flat plate stress intensity factor is

$$k_p = \frac{p_o R}{h}\sqrt{(a)}\ , \qquad (5.85)$$

where p_o is the internal pressure and the dimensions R, h, a are shown in Figure 5.1. Generally the results in cylindrical as well as spherical shells are presented in terms of the dimensionless "shell parameter" λ defined by

$$\lambda = [(12(1-\nu^2)]^{\frac{1}{4}}\, a/\sqrt{(Rh)} \qquad (5.86)$$

in isotropic shells, and

$$\lambda = [12(1-\nu_1\nu_2)E_2/E_1]^{\frac{1}{4}}\, a/\sqrt{(Rh)} \qquad (5.87)$$

in orthotropic shells (see equation (5.20)). It is seen that the parameter λ in the specially orthotropic shells depends on two elastic constants and, therefore, is not an appropriate correlation coefficient to be used for the purpose of comparing the results in two different shells with the same geometry

and different materials. Thus, in Figures 5.2 to 5.5 a purely geometrical parameter, namely $a/\sqrt{(Rh)}$ is used as the independent variable.

Also, from the analysis given in the previous sections it is clear that the dependence of the results on elastic constants is not through λ only. Hence, the orthotropic results shown in the figures are for the specific material constants given in Table 5.1. Similarly, for the isotropic shells the Poisson's ratio ν appears in the analysis through λ as well as elsewhere. The isotropic shell results shown in Figures 5.2 to 5.5 under the designation $(E_1/E_2) = 1$ are thus obtained for one value of ν only, namely $\nu = 1/3$. The effect of ν on the stress intensity factors in isotropic shells is discussed in the following section. In each figure there are two sets of orthotropic results which correspond to the alignment of the stiff direction of the material in the axial or the circumferential direction of the cylinders.

The results indicate that in the specially orthotropic shells the stress intensity factors are strongly dependent on the modulus ratio E_1/E_2, and generally they increase with decreasing E_1/E_2, E_1 being the modulus in axial direction. This does not, of course, necessarily mean a reduction in the resistance of the shell to crack propagation as the shell becomes stiffer in circumferential direction. Any material, particularly a composite, which is not isotropic in elastic properties, would not be expected to be isotropic in its resistance to crack propagation. In each case the load-bearing strength of the structure would, of course, be decided by the ratio of the stress intensity factor or whatever the measure of the severity of the external loads and the crack geometry to the corresponding strength parameter of the material.

Figure 5.6 shows the results for a cylinder with an axial crack under skew symmetric loading. Here it is assumed that the cylinder is under torsion and away from the crack region the uniform shear $N_{xy} = N_o$ is the only nonzero stress component acting on the shell. Thus, the corresponding flat plate stress intensity factor is a mode II component given by $k_p = N_o\sqrt{(a)}/h$. The membrane and bending stress intensity factor ratios C_m and C_b shown in the figure are defined by equations (5.50), (5.51), and (5.54). In this example too $a/\sqrt{(Rh)}$ rather than the shell parameter λ is used as the independent variable and for the isotropic case (designated by $(E_1/E_2) = 1$) it is again assumed that $\nu = 1/3$. Figure 6 shows the same trend as Figures 5.2-5.5, namely, the stress intensity factors increase with decreasing E_1/E_2. This appears to be primarily due to the multiplicative factor $(E_1/E_2)^{\frac{1}{4}}$ in the expression of the shell parameter λ given by equation (5.85). In fact for a quick estimate of the stress intensity ratios in skew-symmetric as well as in symmetric problems for the specially orthotropic shells the isotropic results may be sufficient provided λ is calculated from equation (5.87).

Table 5.2, which shows the results for only one value of the variable $a/\sqrt{(Rh)} = 1.66$, gives some idea about the relative effect of material orthotropy. Here the results for graphite, titanium, and an isotropic material ($\nu = 1/3$) are compared. In this case too, the strong influence of material orthotropy is apparent.

Table 5.2 The effect of orthotropy on the stress intensity ratios ($a/\sqrt{(Rh)} = 1.66$)

	Isotropic Material	Titanium		Graphite	
E_1/E_2	1.0	1.381	0.724	26.667	0.0375
λ	3.0	2.811	3.304	1.359	7.018
C_m	1.942	1.880	2.044	1.340	4.045
C_b	0.199	0.158	0.239	0.019	1.241

5.6 The Effect of Poisson's Ratio

As indicated in the previous section, in the isotropic shells the Poisson's ratio ν appears in the analysis explicitly as well as through λ defined by equation (5.86). This means that the stress intensity factors are functions of two independent variables, namely ν and $a/\sqrt{(Rh)}$. However, since in most metallic structural materials ν is in the neighborhood of 1/3 and since ν affects the results partly if not mostly through λ, in practice the tendency has been to present the results by using only λ as the independent variable for a fixed Poisson's ratio, $\nu = 1/3$. To justify this or to throw some light on the approximation involved, the effect of ν for some selected values of λ or $a/\sqrt{(Rh)}$ has to be studied.

Figures 5.7 to 5.9 show some results for a cylindrical shell with an axial crack. Figure 5.7 show the variation of the symmetric stress intensity factor ratios A_m and A_b for $\lambda = 1$ and $\lambda = 3$ in a pressurized cylinder where

$$A_m = \frac{k_s^m}{k_p}, \quad A_b = \frac{k_s^b}{k_p}, \quad k_p = \frac{N_o\sqrt{a}}{h} = \frac{p_o R\sqrt{a}}{h} . \tag{5.88}$$

In this case the effect of ν on the main stress intensity component A_m appears

to be negligible. Figure 5.8 shows some symmetric results for the shell under cylindrical bending only in which $M_{yy} = - M_o$ is the only nonzero crack surface loading. For this loading the corresponding flat plate stress intensity factor is defined by

$$k_p = \frac{6M_o}{h^2}\sqrt{a} \tag{5.89}$$

and A_m and A_b are again given by equations (5.88). In this case too the variation of the main stress intensity component A_b with ν for the values of $\lambda = 1$ and $\lambda = 3$ does not appear to be significant. Even though there is a considerable relative change in A_m as ν goes from zero to 0.5, it should be observed that the absolute value of A_m itself is rather small.

An example for the skew-symmetric problem is shown in Figure 5.9. Here it is assumed that a cylinder containing an axial crack is under torsion and $\lambda = 5$. The related stress intensity factors are defined by equations (5.50), (5.51), and (5.54). For this λ value, the effect of ν again appears to be negligible.

It should be noted that in Figures 5.7 to 5.9 λ is used as a constant parameter. Since λ is a decreasing function of ν, this would compensate some of the increases in the stress intensity factor ratios observed for increasing ν. A somewhat more meaningful result would be obtained by comparing the stres intensity factor ratios for different Poisson's ratios and a fixed geometric parameter $a/\sqrt{(Rh)}$. A very limited such comparison for the symmetric problem is shown in Table 5.3 which leads to the same general conclusion that the effect of ν on the stress intensity factors is not very significant.

Table 5.3 The effect of Poisson's ratio

$\frac{a^2}{Rh}$	ν	$N_o \neq 0,\ M_o = 0$		$N_o = 0,\ M_o \neq 0$	
		A_m	A_b	A_m	A_b
0.3	0.5	2.157	0.353	0.097	0.810
	1/3	2.163	0.364	0.078	0.865
2.63	0.15	2.066	0.352	0.057	0.912
	1/3	2.074	0.370	0.076	0.873
2.6	0	2.045	0.326	0.043	0.932
	1/3	2.059	0.372	0.076	0.875

5.7 Interaction of Two Cracks

In plane problems it is known that if the medium contains more than one crack, depending on the relative distance between the cracks, there could be a strong interaction between the respective stress fields and the stress intensity factors could be highly affected. In order to give some idea about the effect of interacting stress fields on the stress intensity factors in shells, in this section the results of a simple problem for a pressurized cylindrical shell containing two axial cracks are presented. From the formulation and the solution of the crack problem in shells given in Sections 2-4 of this chapter it is clear that there is no major difficulty in formulating the problem and in deriving the governing system of singular integral equations if the shell contains, instead of a single crack, a set of collinear cracks. Therefore, there is no need to present further analytical details.

In the example under consideration the two cracks are assumed to be equal in length. The particular crack geometry and dimensions are shown by the insert in Figure 5.10, and the results are shown in Figures 5.10 and 5.11. The stress intensity factor ratios A_m and A_b are again defined by equations (5.88). The superscripts i and o on A_m and A_b refer to the inner and outer crack tips, respectively. The figures show the results for $\lambda = 1,2,3$ where λ is defined by equation (5.86) and ν again is assumed to be 1/3. For the purpose of comparison, Figure 5.10 also shows the stress intensity factor ratios for the flat plate with the same crack geometry evaluated from [25]

$$A_m^i = \frac{k_p^i}{k_p} = \frac{b_1^2 E(m)/K(m) - a_1^2}{(b_1 - a_1)[a_1(b_1+a_1)/2]^{\frac{1}{2}}} , \tag{5.90a}$$

$$A_m^o = \frac{k_p^o}{k_p} = \frac{b_1^2[1 - E(m)/K(m)]}{(b_1 - a_1)[b_1(b_1+a_1)/2]^{\frac{1}{2}}} , \tag{5.90b}$$

where

$$k_p = \frac{p_o R\sqrt{a}}{h} , \quad a_1 = c - a , \quad b_1 = c + a , \quad m = 1 - \frac{a_1^2}{b_1^2} , \tag{5.91}$$

and K(m) and E(m) are the complete elliptic integrals of the first and the second kind, respectively.

For $a/c = 0$ the two cracks are far apart, there is no interaction, and the results correspond to that of a single crack in a pressurized cylinder. On the other hand as $a/c \to 1$, i.e., as the length of the net ligament between the two cracks approaches zero, as expected, the stress intensity factor at the inner crack tip goes to infinity and that at the outer tip approached the value obtained for a single crack of length 4a. However, for $a/c > 0.4$ and

$\lambda \geq 2$ the results show a somewhat unexpected behavior. In flat plates A_m^i is always greater than A_m^o, whereas in shells the results show that for certain ranges of a/c and λ it is possible to have $A_m^i < A_m^o$. This behavior seems to be even more pronounced for the bending stress intensity factors shown in Figure 5.11. A partial explanation of this phenomenon may be found in the distribution of the displacement component w(x,y) normal to the shell surface. In a pressurized isotropic shell containing a single crack of length 2a, evaluating w in the plane of the crack, i.e., for $x > 0$, $y = 0$, one obtains, for example for $\lambda = 2$, the result shown in Figure 5.12 (where, in the notation of Figures 5.1 and 5.10, $w > 0$ inward). The normalization factor which appears in the figure is given by

$$c_w = \frac{p_o R^2 \lambda^2}{2Eh}, \tag{5.92}$$

and the coordinate x is normalized with respect to a. The figure shows that, although around the crack there is an outward bulging in the shell, further along the x axis w changes sign and there is a zone of depression. When the distance c is small enough for the stress and displacement fields of the two cracks to interact, for a certain range of c this "depression" may cause a reduction in the stress intensity factors.

5.8 Further Results for Isotropic Shells

This section presents a summary of the calculated results for the three idealized crack geometries, namely a cylindrical shell with an axial crack, that with a circumferential crack, and a spherical shell with a meridional crack. The loading condition is assumed to be homogeneous and either symmetric or skew-symmetric. The Poisson's ratio of 1/3 is assumed in all

calculations. The technique used to solve the related shell problems is similar to that described in Sections 5.3 and 5.4 of this chapter [6-9].

Figures 5.13 and 5.14 show, respectively, the membrane and bending stress intensity factor ratios A_m and A_b for the three shell geometries. In this symmetric case the only nonzero crack surface traction is assumed to be $N_{yy} = -N_o = \text{constant}$, x being the coordinate along the crack.* The results for the symmetric problem in which $M_{yy} = -M_o = \text{constant}$ is the only nonzero crack surface load are given in Figures 5.15 and 5.16. Finally, Figures 5.17 and 5.18 show the skew-symmetric results for the three crack geometries where $N_{xy} = -N_o = \text{constant}$ is the nonzero crack surface traction. In presenting these results λ is defined by equation (5.86), A_m and A_b are defined by equations (5.88) (with k_p as given by equations (5.89) for Figures 5.15 and 5.16), and C_m and C_b are defined by equations (5.50), (5.51), and (5.54).

*It should be noted that there was a numerical error in A_b for the cylindrical shell with a circumferential crack given in [7].

References

1. Copley, L. G. and Sanders, J. L., Jr., A longitudinal crack in a cylindrical shell under internal pressure, *Int. J. Fracture Mechanics*, 5, pp. 117-131 (1969).

2. Duncan, M. E. and Sanders, J. L., Jr., The effect of circumferential stiffener on the stress in a pressurized cylindrical shell with a longitudinal crack, *Int. J. Fracture Mechanics*, 5, pp. 133-155 (1969).

3. Folias, E. S., An axial crack in a pressurized cylindrical shell, *Int. J. Fracture Mechanics*, 1, pp. 104-113 (1965).

4. Folias, E. S., A finite line crack in a pressurized spherical shell, *Int. J. Fracture Mechanics*, 1, pp. 20-46 (1965).

5. Folias, E. S., A circumferential crack in a pressurized cylinder, *Int. J. Fracture Mechanics*, 3, pp. 1-12 (1967).

6. Erdogan, F. and Kibler, J. J., Cylindrical and spherical shells with cracks, *Int. J. Fracture Mechanics*, 5, pp. 229-237 (1969).

7. Erdogan, F. and Ratwani, M., Fatigue and fracture of cylindrical shells containing a circumferential crack, *Int. J. Fracture Mechanics*, 6, pp. 379-392 (1970).

8. Erdogan, F and Ratwani, M., Plasticity and crack opening displacement in shells, *Int. J. Fracture Mechanics*, 8, pp. 413-426 (1972).

9. Erdogan, F. and Ratwani, M., A circumferential crack in a cylindrical shell under torsion, *Int. J. Fracture Mechanics*, 8, pp. 87-95 (1972).

10. Murthy, M. V. V., Rao, K. P., and Rao, A. K., Stresses around an axial crack in a pressurized cylindrical shell, *Int. J. Fracture Mechanics*, 8, pp. 287-297 (1972).

11. Murthy, M. V. V., Rao, K. P., and Rao, A. K., On the stress problem of large elliptical cutouts and cracks in circular cylindrical shells, *Int. J. Solids Structures*, 10, pp. 1243-1269 (1974).

12. Erdogan, F. and Ratwani, M., A note on the interference of two collinear cracks in a cylindrical shell, *Int. J. of Fracture*, 10, pp. 463-465 (1974).

13. Erdogan, F. and Ratwani, M., Fracture of cylindrical and spherical shells containing a crack, *Nuclear Engineering and Design*, 20, pp. 265-286 (1972).

14. Yuceoglu, U. and Erdogan, F., A cylindrical shell with an axial crack under skew-symmetric loading, *Int. J. Solids Structures*, 9, pp. 347-362 (1973).

15. Erdogan, F., Ratwani, M., and Yuceoglu, U., On the effect of orthotropy in a cracked cylindrical shell, *Int. J. of Fracture*, 10, pp. 369-374 (1974).

16. Yuceoglu, U., Ph.D. Dissertation, Lehigh University (1971).

17. Hartranft, R. J. and Sih, G. C., Effect of plate thickness on the bending stress distribution around through cracks, *J. of Mathematics and Physics*, 47, pp. 276-291 (1969).

18. Ambartsumyan, S. A., On the theory of anisotropic shallow shells, NACA Tech. Memo. 1424 (1956).

19. Ambartsumyan, S. A., Theory of anisotropic shallow shells, NASA Tech. Transl. F-118 (1964).

20. Flügge, W. and Conrad, D. A., Singular solutions in the theory of shallow shells, Tech. Report No. 101, Stanford University (1956).

21. Apeland, K., Analysis of anisotropic shallow shells, *Acta Technica Scandinavica*, 22 (1963).

22. Muskhelishvili, N. I., *Singular Integral Equations*, P. Noordhoff, Groningen (1953).

23. Erdogan, F., Gupta, G. D., and Cook, T. S., Numerical solution of singular integral equations, in *Methods of Analysis and Solutions of Crack Problems*, G. C. Sih, ed., Noordhoff International Publishing, Leyden (1973).

24. Gradshteyn, I. S. and Ryzhik, I. M., *Tables of integrals, series and products*, Academic Press (1965).

25. Erdogan, F., On the stress distribution in plates with collinear cuts under arbitrary loads, *Proc. 4th U.S. Nat. Cong. Appl. Mech.*, 1, pp. 547-553 (1962).

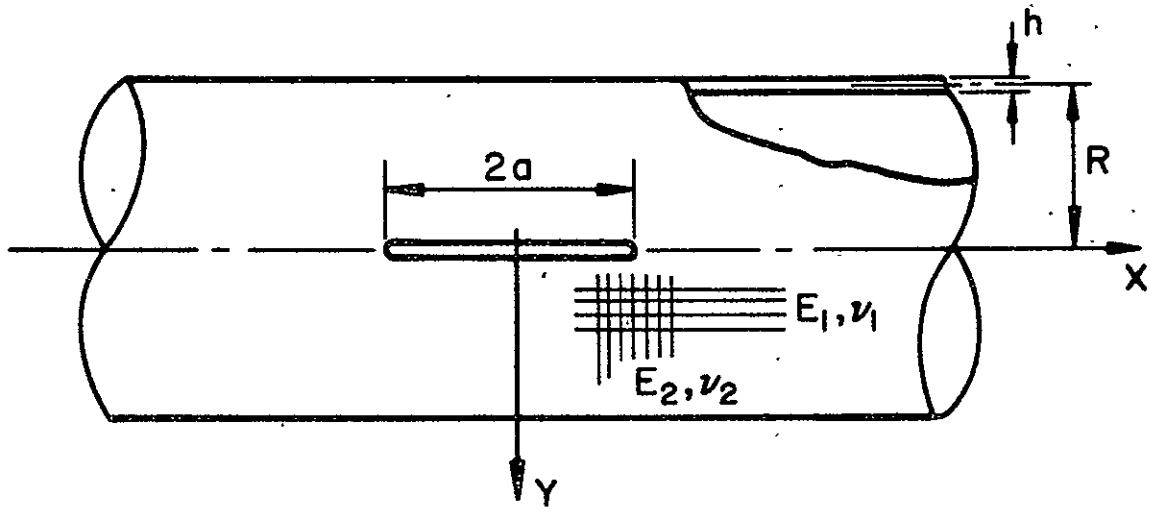

Figure 1. Geometry of a cylindrical shell with an axial crack.

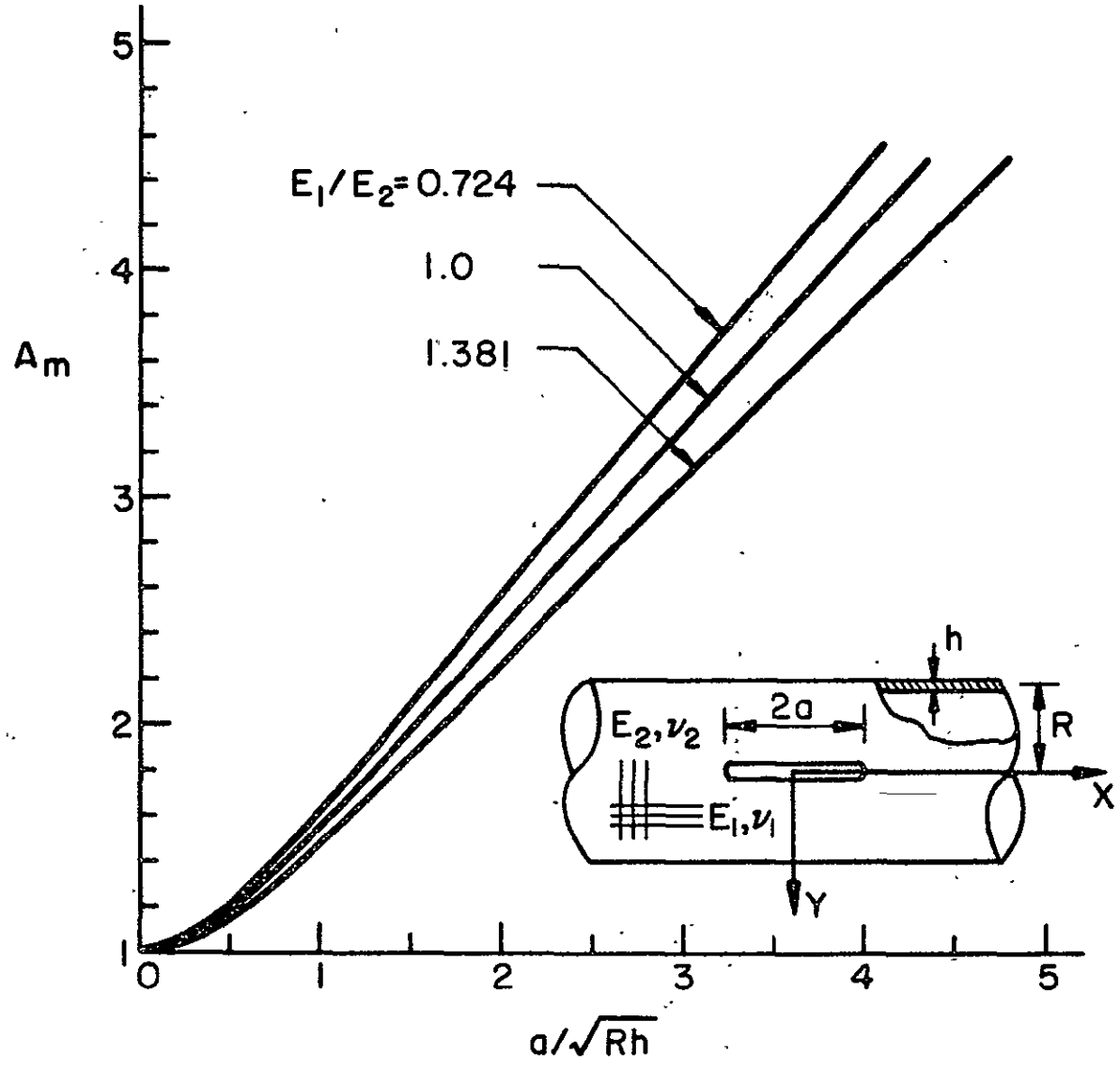

Figure 2. Membrane component of the stress intensity factor ratio A_m for a pressurized Titanium and for an isotropic ($\nu = 1/3$) cylinder.

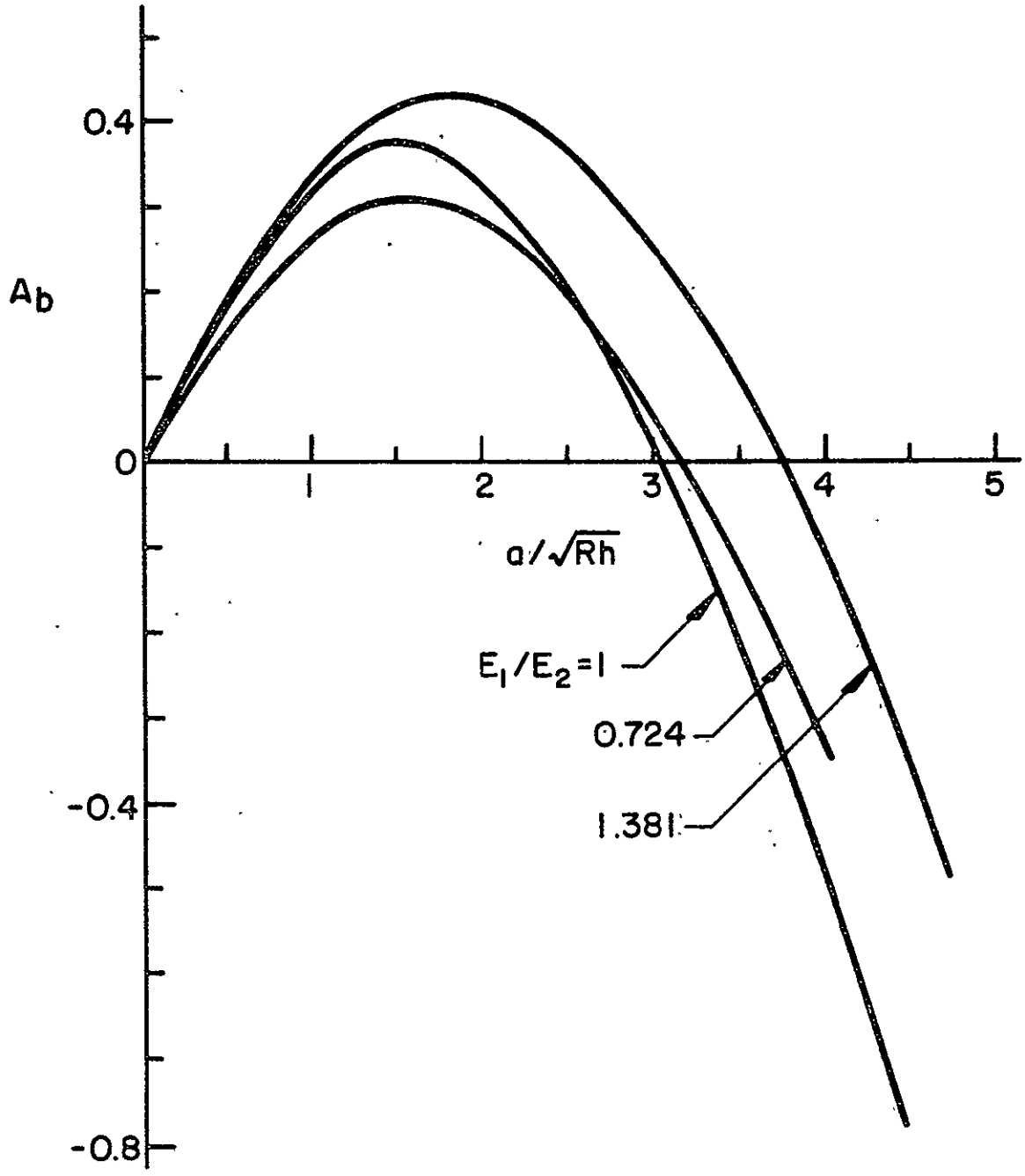

Figure 3. Bending component of the stress intensity factor ratio A_b for a pressurized Titanium and for an isotropic cylinder.

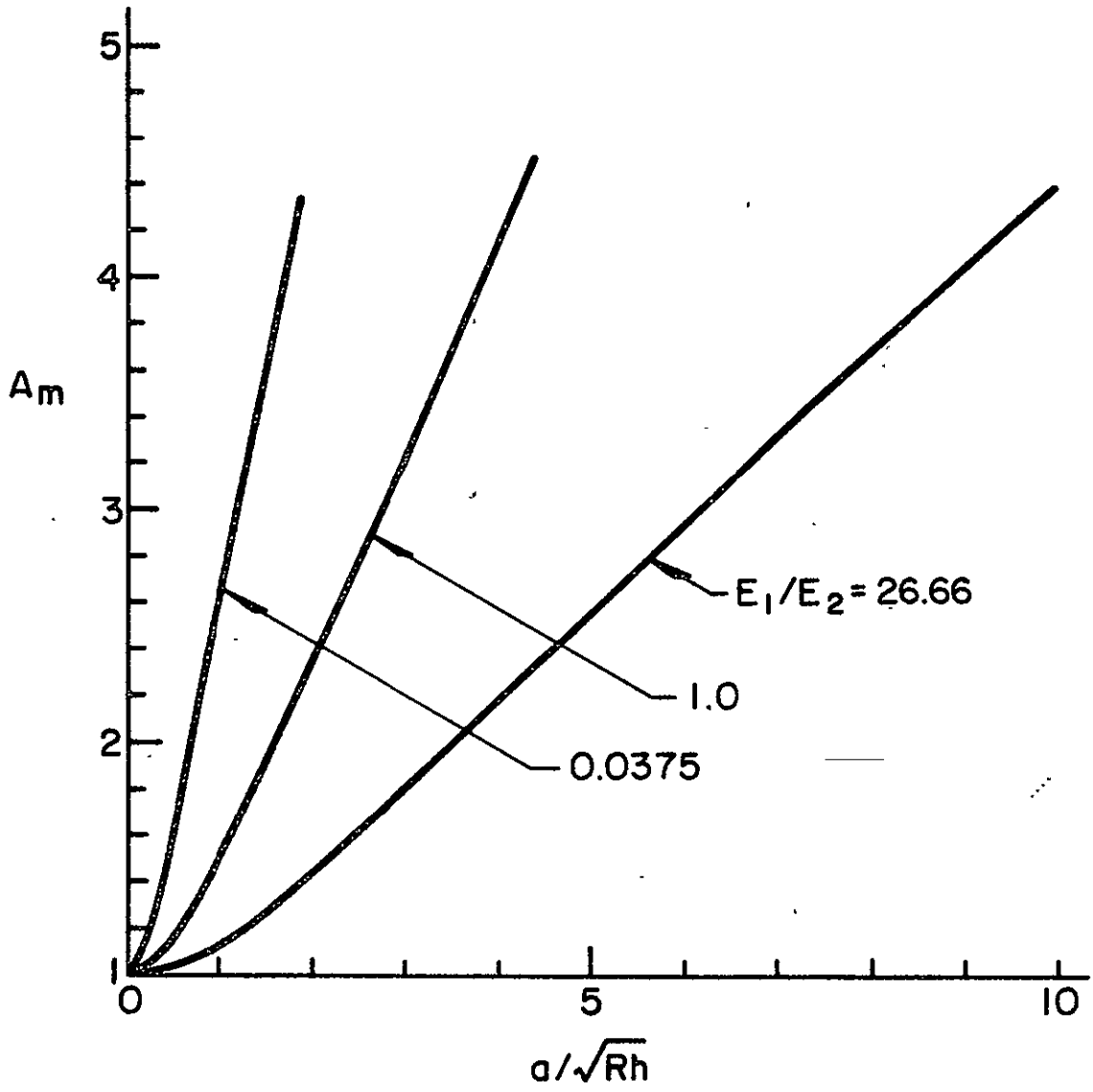

Figure 4. Membrane component of the stress intensity factor ratio A_m for a pressurized Graphite and for an isotropic cylinder.

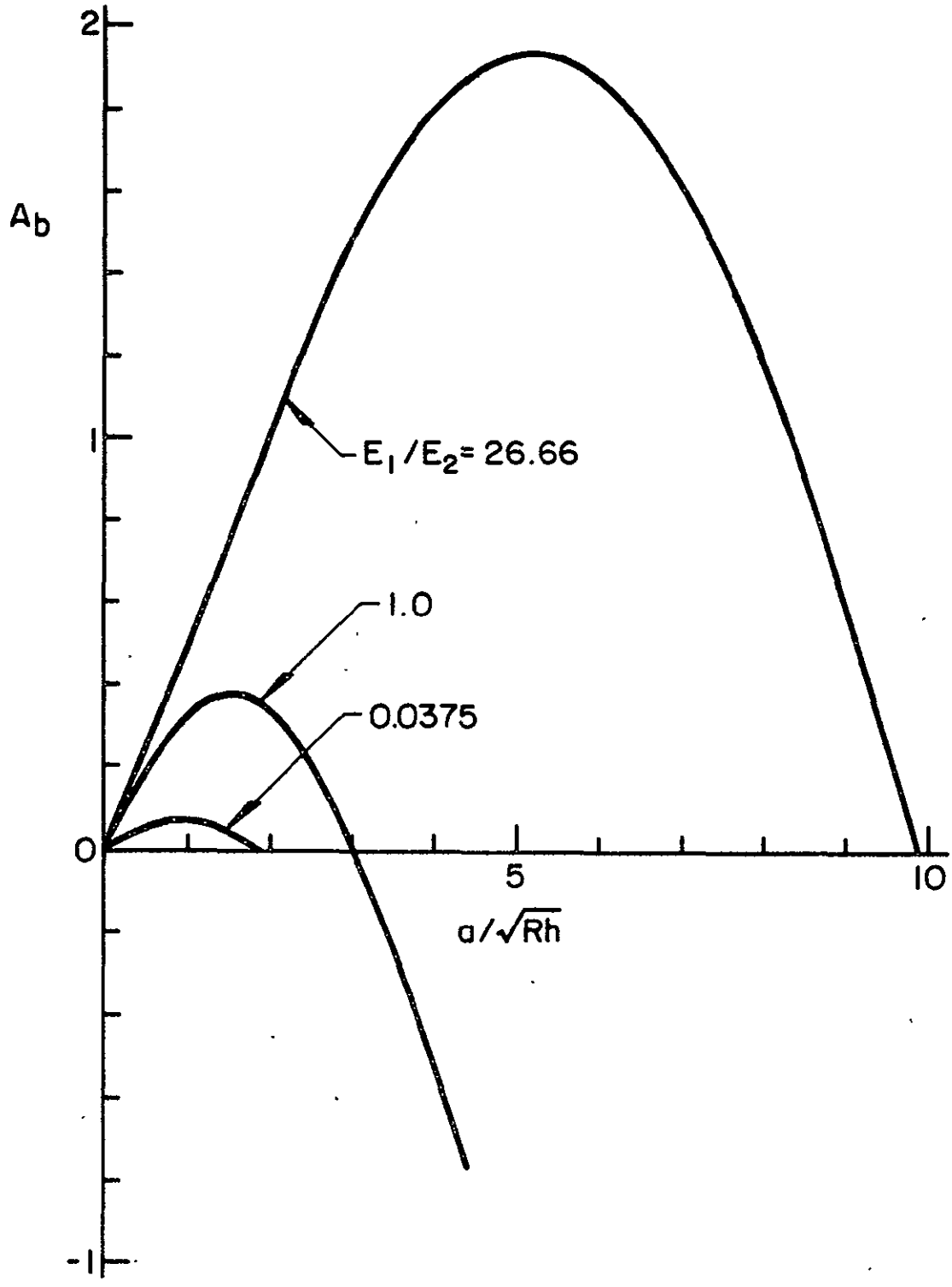

Figure 5. Bending component of the stress intensity factor ratio A_b for a pressurized Graphite and for an isotropic cylinder.

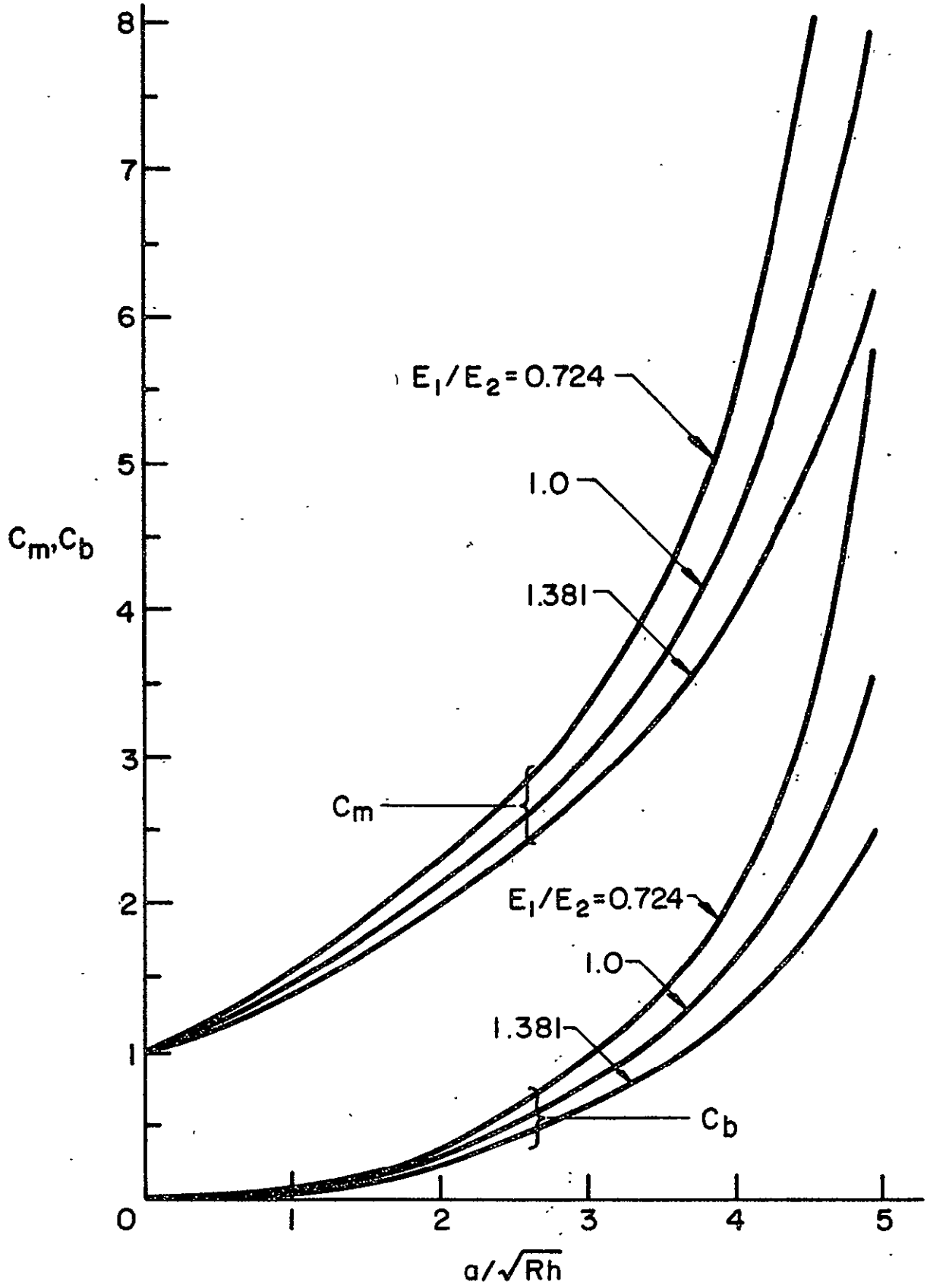

Figure 6. Membrane and bending components of the stress intensity factor ratio, C_m and C_b for a specially orthotropic (Titanium) and for an isotropic ($\nu = 1/3$) cylinder under torsion.

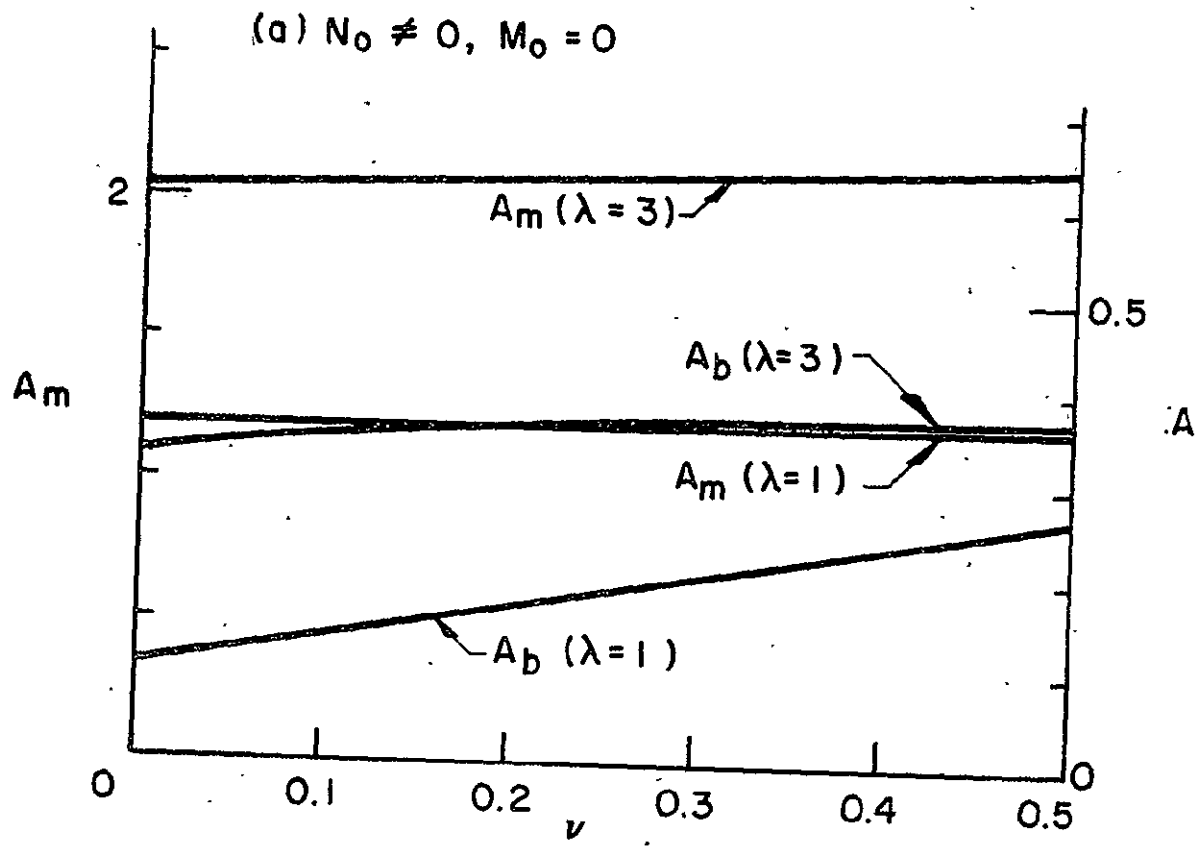

Figure 7. The effect of Poisson's ratio on the stress intensity factors in a pressurized isotropic cylinder with an axial crack.

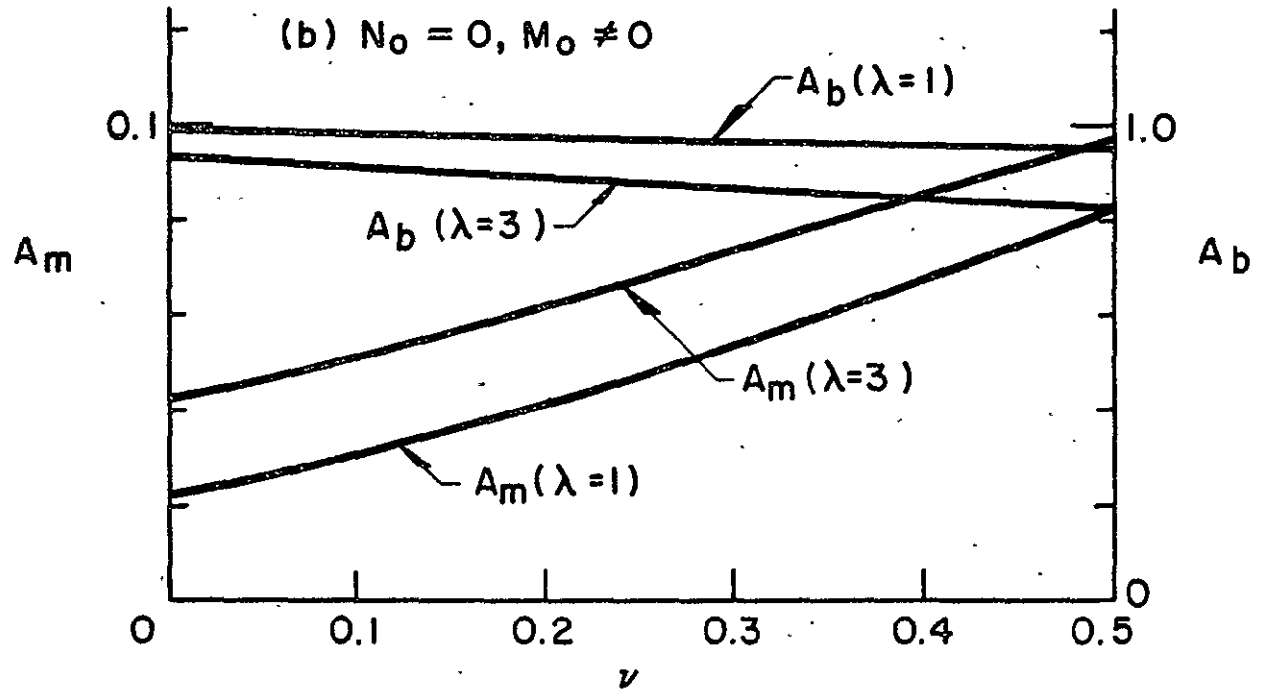

Figure 8. The effect of Poisson's ratio on the stress intensity factors in an axially cracked cylindrical shell under uniform bending, $M_{yy} = M_o$.

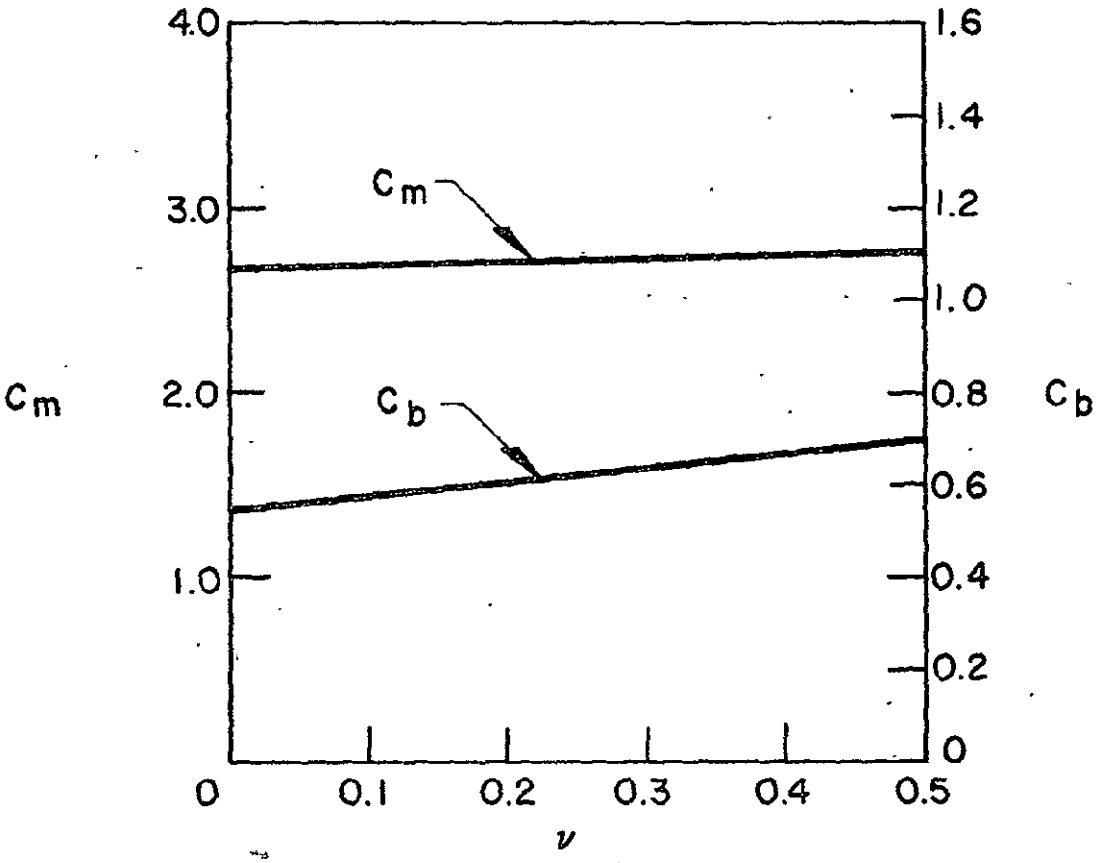

Figure 9. The effect of Poisson's ratio on the stress intensity factors in an axially cracked isotropic cylinder under torsion ($\lambda = 5$).

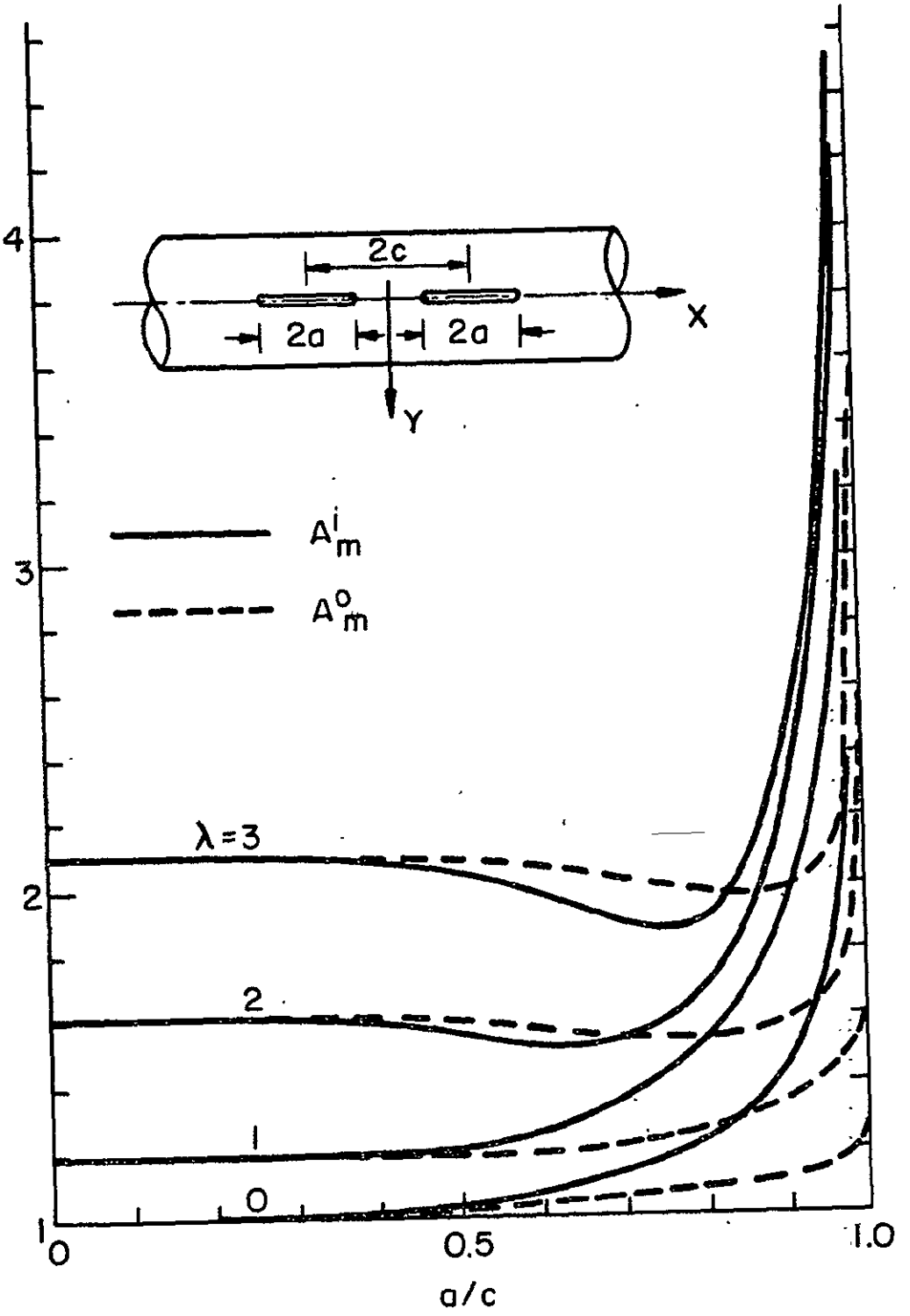

Figure 10. The membrane components of the stress intensity factor ratio in a pressurized isotropic cylinder ($\nu = 1/3$) with two collinear axial cracks. A^i_m for the inner crack tip, A^o_m for the outer crack tip.

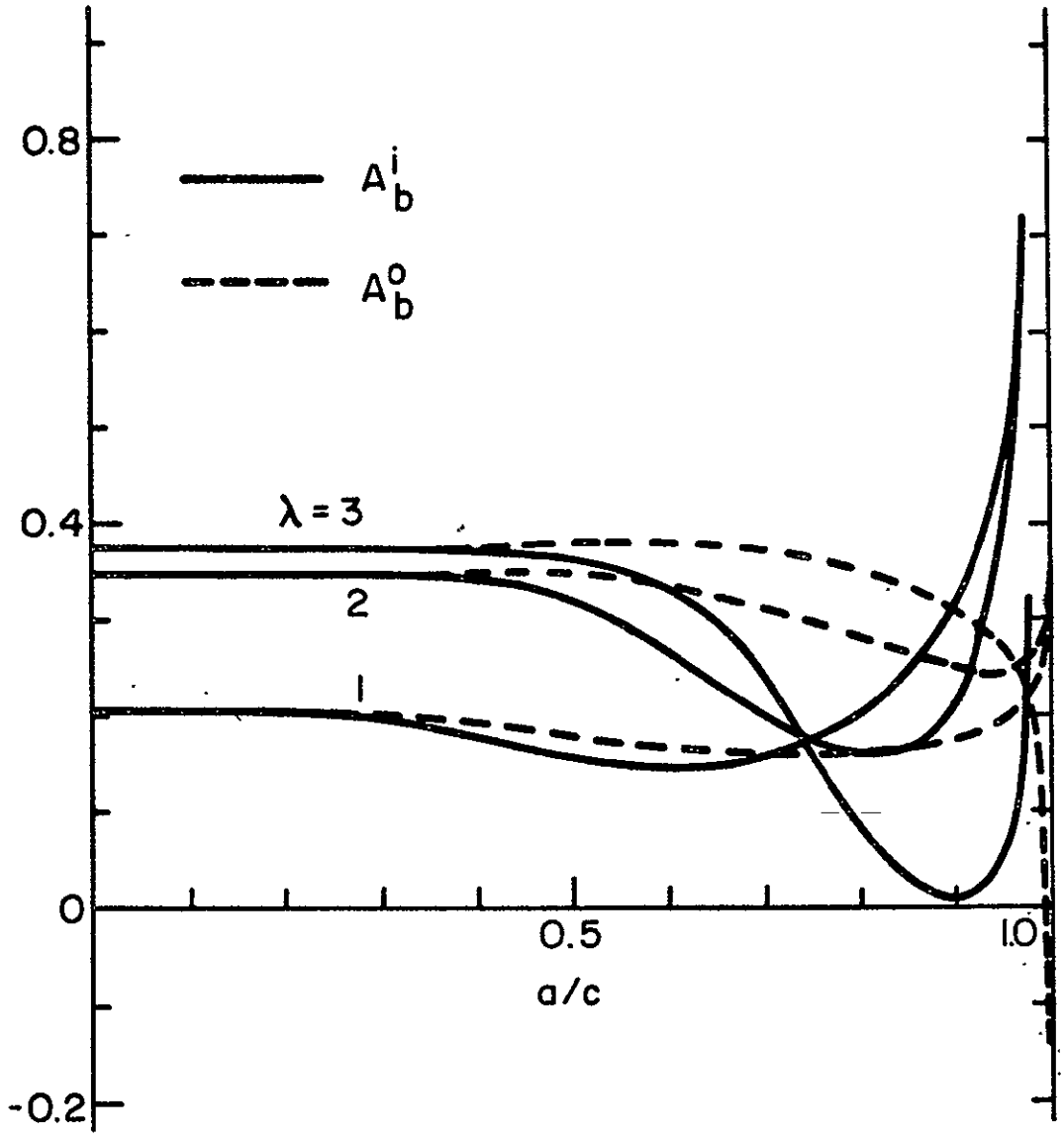

Figure 11. The bending components of the stress intensity factor ratio in a pressurized cylinder with two axial cracks. A_b^i for the inner crack tip, A_b^o for the outer crack tip.

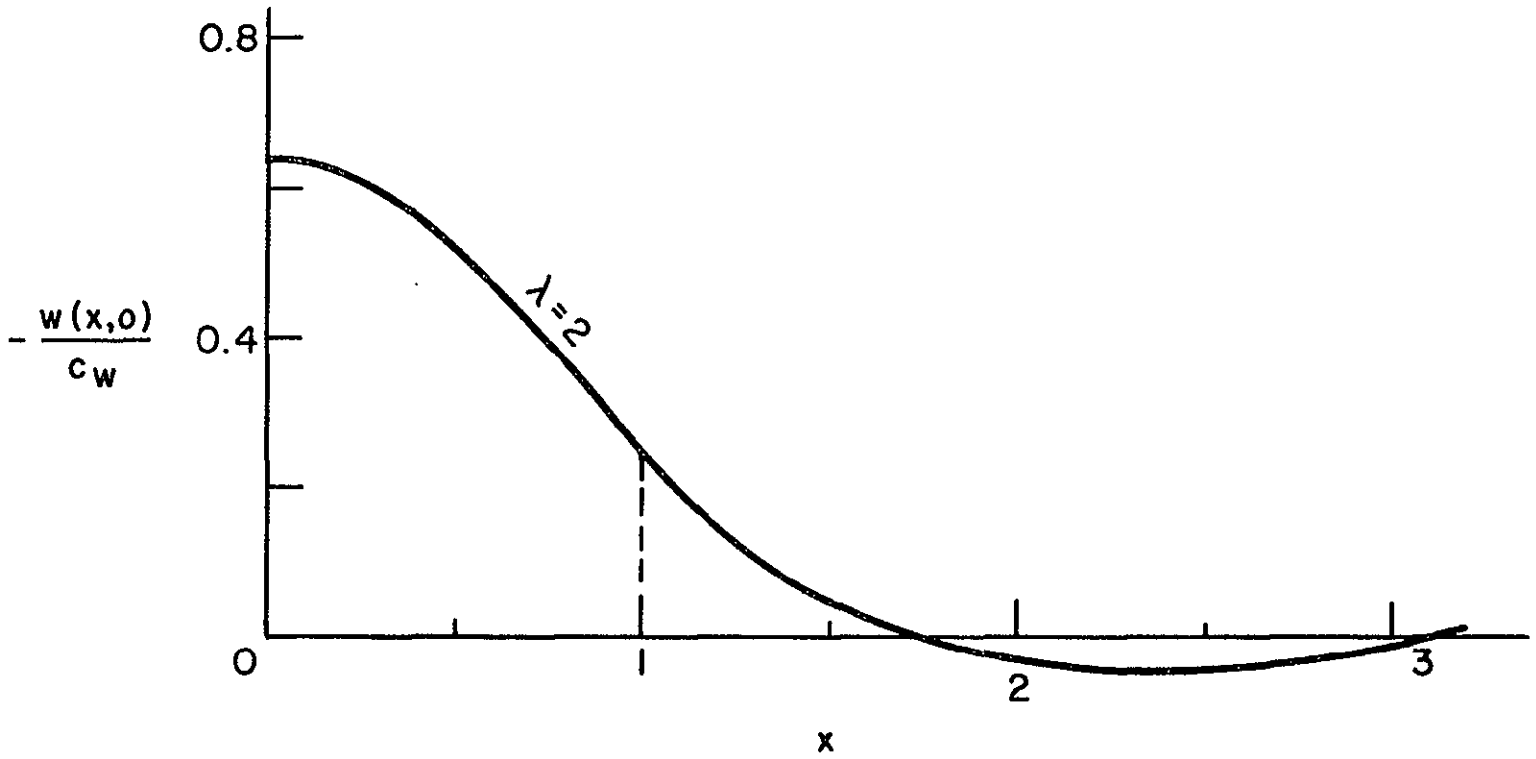

Figure 12. Displacement component w normal to the shell surface in the plane of the crack for a pressurized cylinder with an axial crack, x = X/a.

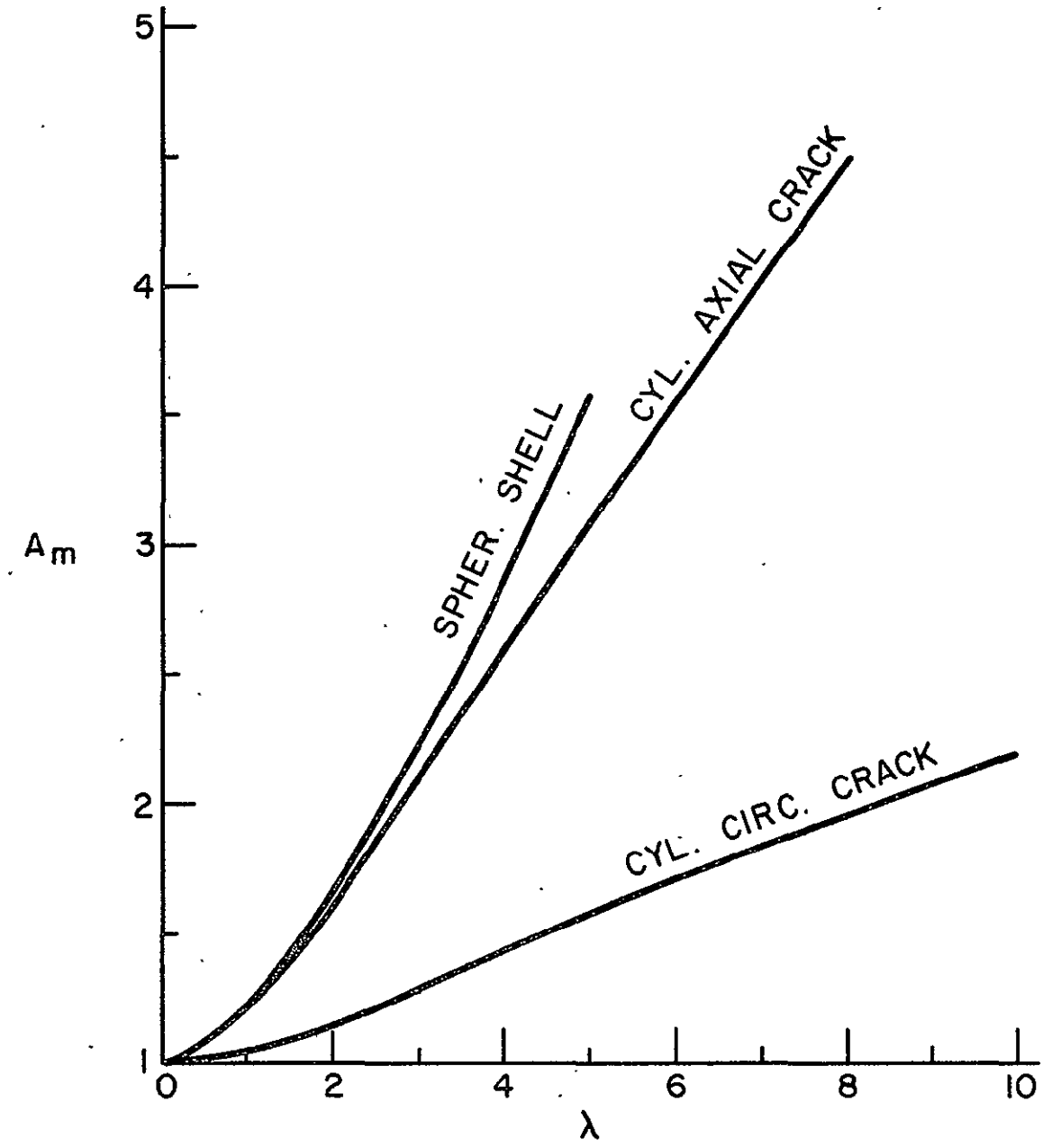

Figure 13. Membrane component of the stress intensity factor ratio in symmetrically-loaded shells: $N_{yy} = N_0 \neq 0$, $M_{yy} = 0$.

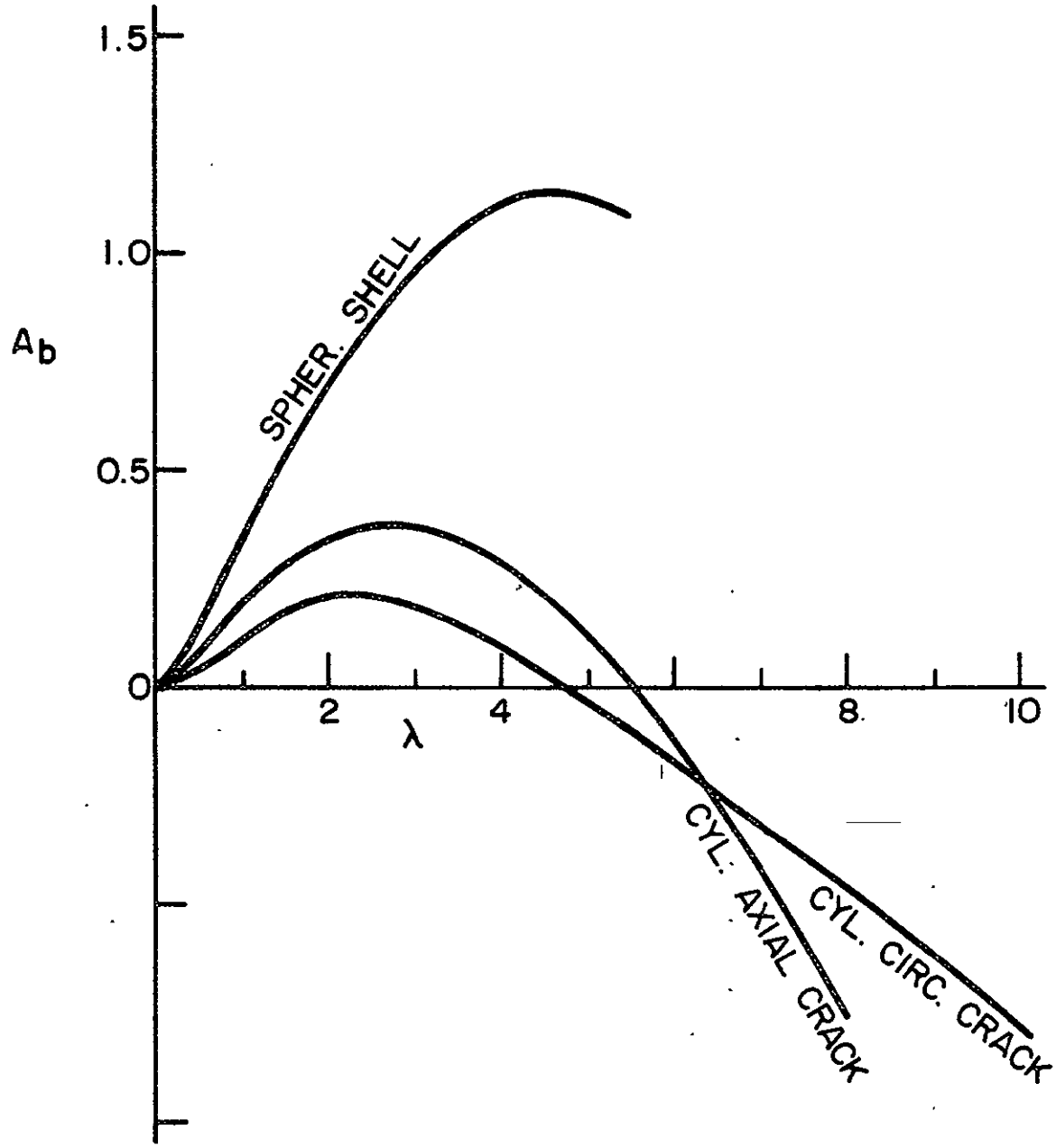

Figure 14. Bending component of the stress intensity factor ratio in symmetrically-loaded shells: $N_{yy} = N_0 \neq 0$, $M_{yy} = 0$.

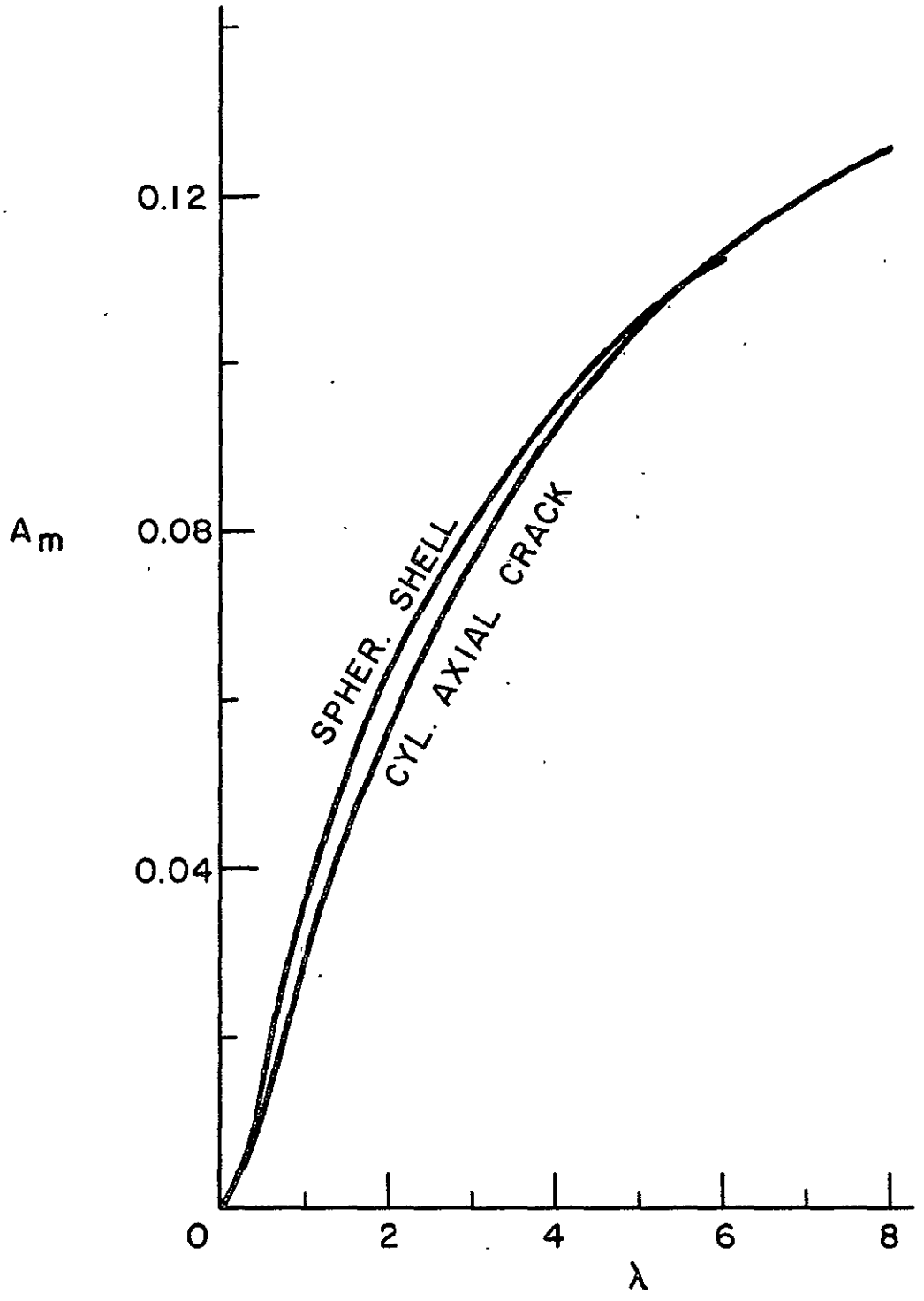

Figure 15. Membrane component of the stress intensity factor ratio in shells symmetrically-loaded in bending: $M_{yy} = M_0 \neq 0$, $N_{yy} = 0$.

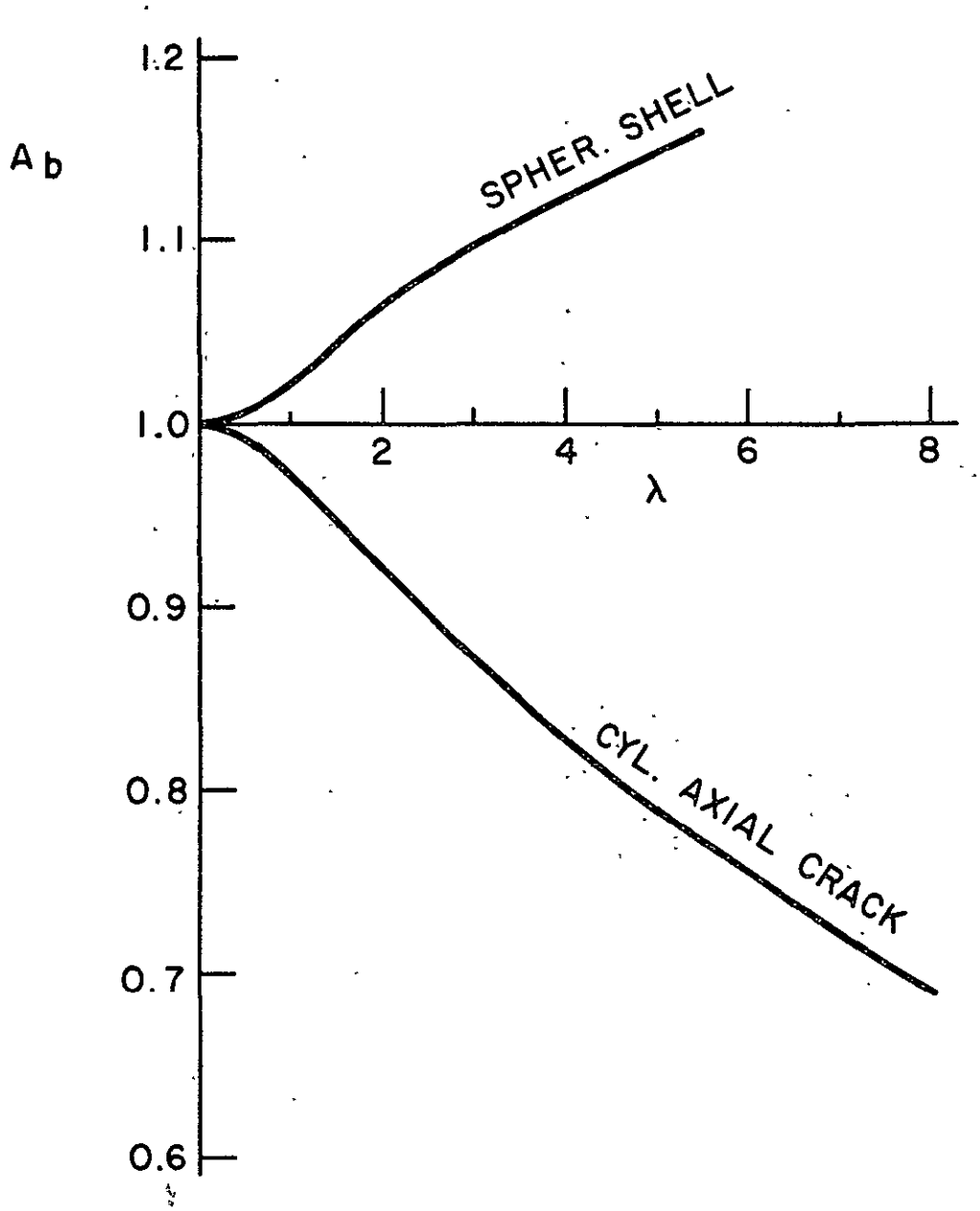

Figure 16. Bending component of the stress intensity factor ratio in shells symmetrically loaded in bending: $M_{yy} = M_0 \neq 0$, $N_{yy} = 0$.

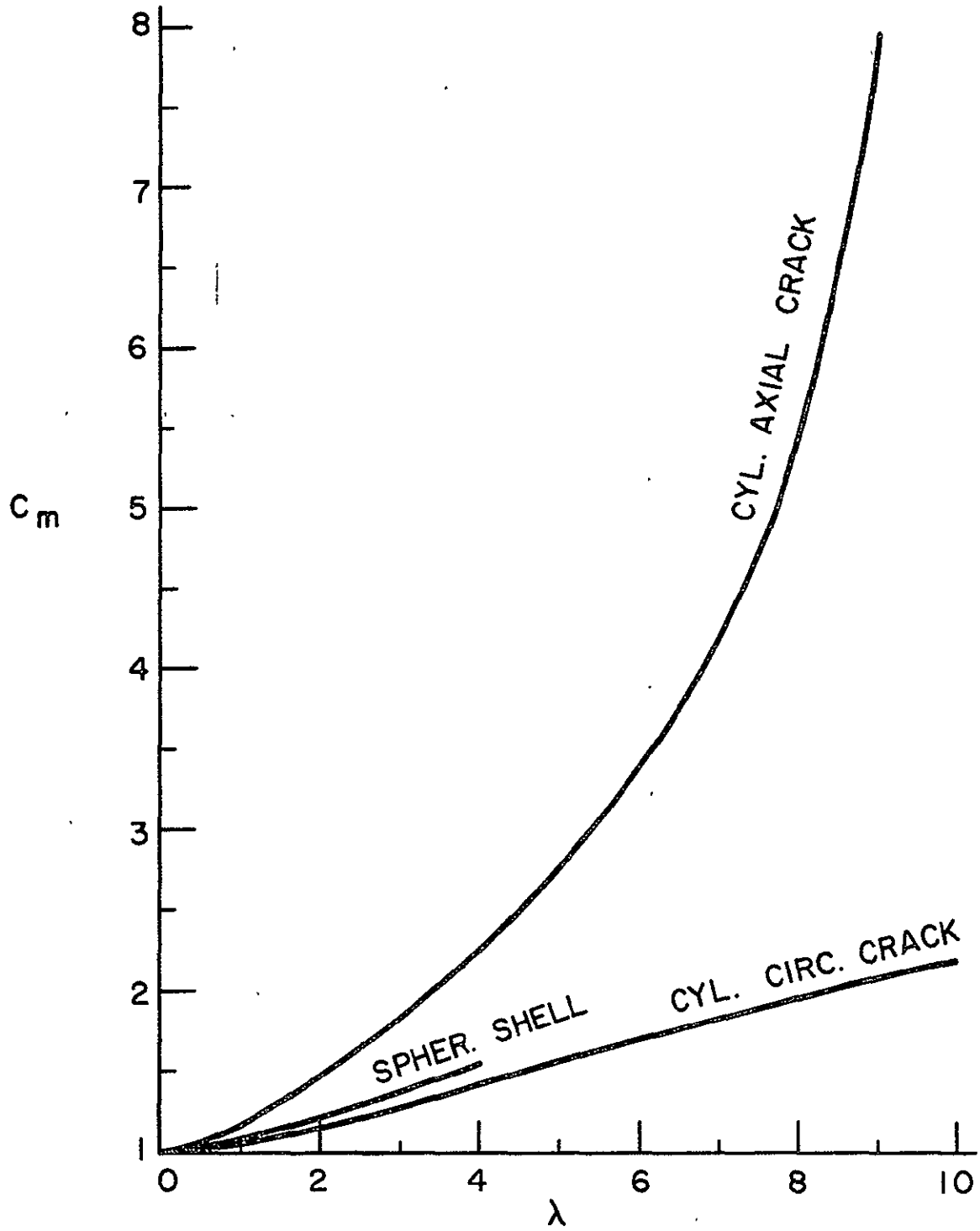

Figure 17. Membrane component of the stress intensity factor ratio in shells under uniform skew-symmetric membrane loading: $N_{xy} = N_0$.

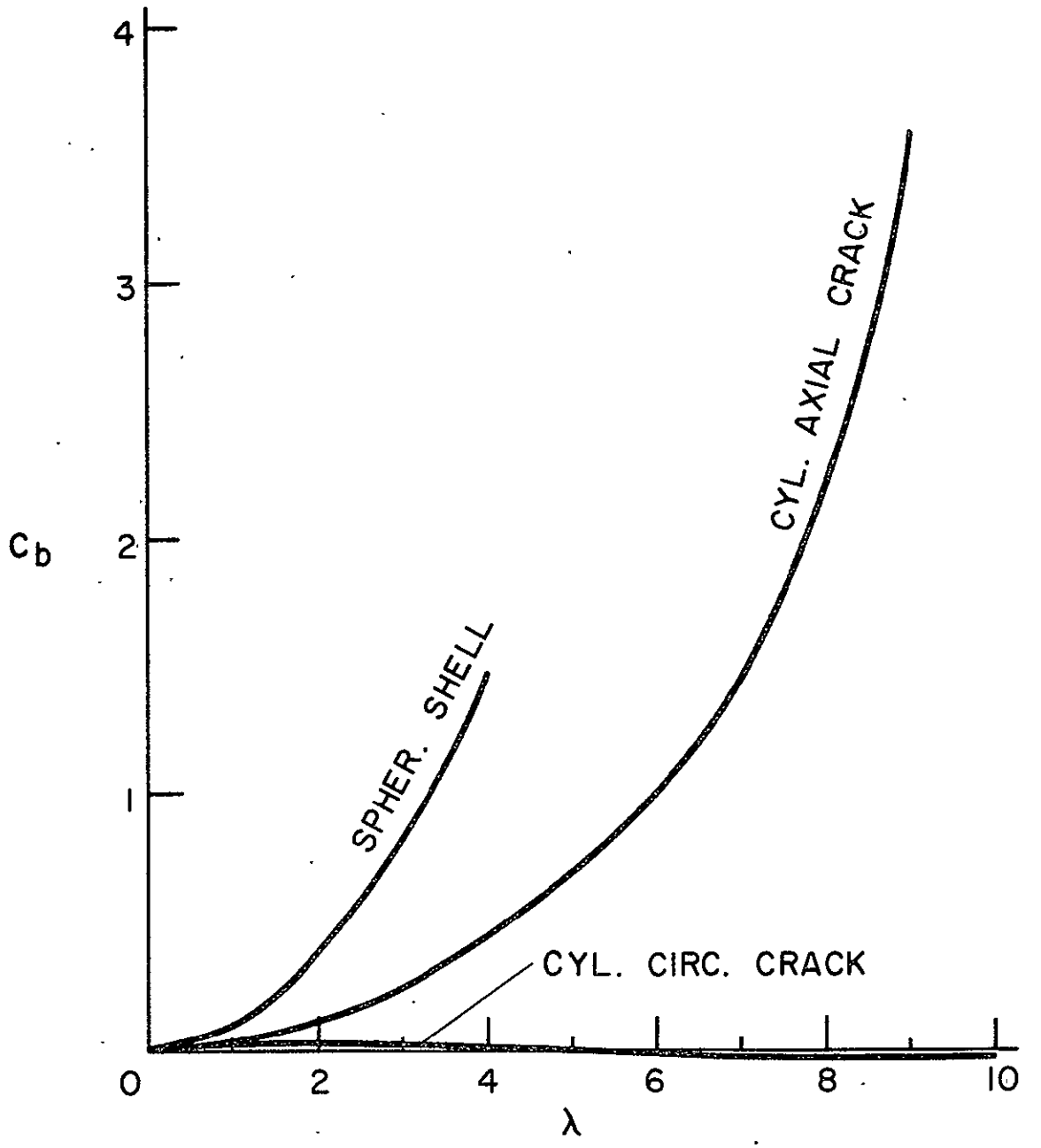

Figure 18. Bending component of the stress intensity factor ratio in shells under uniform skew-symmetric membrane loading: $N_{xy} = N_0$.